Development and Validation of the Actuation and Control System for a Gut-on-Chip Device

by
Kyriaki Kekkou

Submitted to the University of Cyprus in partial fulfillment of the requirements for the degree of Masters of Science in Electrical Engineering

Department of Electrical and Computer Engineering

June 2024

Development and Validation of the Actuation and Control System for a Gut-on-Chip Device

by
Kyriaki Kekkou

Examination committee:

Chrysafis Andreou
Assistant Professor, Department of ECE, Advisor

Constantinos Pitris
Professor, Department of ECE, Committee Member

Margarita Chli
Assistant Professor, Department of ECE, Committee Member

Abstract

Organs-on-chip are microfluidic devices that recapitulate the micro-environment of biological tissues. They offer a platform to study the organ's physiology, in health and disease, and enable highly controlled experiments for therapeutics, drugs, as well as more basic biological studies. This technology can replace animal testing, which is clearly a cruel, unethical, and ineffective way to carry out experiments. It has been established that results from animal tests are unreliable due to the differences between them and the human body. Additionally, organ-on-chip platforms are cost-effective and easily customizable. This work focuses on the development of a "Gut-on-a-chip". Gastrointestinal (GI) cancer makes up 26% of the new cancer cases worldwide. GI cancer is one of the biggest challenges that the modern world has to face and its early detection and treatment are among the priorities of the cancer research community. Through this work, we built the hardware related to a gut-on-a-chip device. Specifically, we designed and fabricated the microfluidic device using soft lithography and 3D printing, as well as the pneumatic and fluidic controls to actuate the device. The mechanical actuation was measured using optical microscopy and image processing.

Acknowledgments

I would like to express my gratitude to all the people that have supported me in any way, throughout this work and believed in me and my abilities. First of all, I want to give a special thanks to my professor, Dr. Chrysafi Andreou for giving me the opportunity to work with him and be inspired by his own work and passion about Biomedical Engineering. During these years, his constant support and guidance with patience and empathy, have empowered me to learn and try so many new things and strive for the best even if sometimes things weren't going as expected. I want to also give a big thanks to Dr. Mario Stavrou, he has taught me so many things and he was always willing to assist me. His help was very valuable and I really appreciate everything he has done.

Additionally, I want to express my great appreciation to my support system, my family, my friends and my boyfriend. In order for me to focus on my studies, my family selflessly has provided everything they could to support me, and they never cease to believe in me and what I can achieve. Also, my boyfriend and my friends have been supporting and encouraging me in every step of the way, their presence in my life made everything more beautiful and bearable. Lastly, I am forever grateful for my dog and his unconditional love.

Contents

List of Figures

Chapter 1

Introduction

This project, started having in our minds the struggles and the pain that patients of cancer and their families go through. Gut cancer is one of the most common type of cancer consisting of 26% of the new cancer cases and 35% of deaths worldwide. Colorectal cancer, as one of the many gut cancers, is the third most common type of cancer and lately it affects more and more younger people. This alarming increase of the fatalities, has gain the attention of the research community, since there is an urgent need for a better tools for earlier detection and treatment.

Till now, experiments for new drugs and therapeutics were carried out using animal tests that more times that not, they led to failure during the next step of clinical trials, with a lot of waste of money, resources and a valuable time. Animal tests, cannot provide accurate and reliable results, since beyond the few similarities between the organisms there is no other animal that resembles the human body. Besides, using animals for experiments, many times cause them stress and harm which is cruel and unethical. The animal experiments should be immediately banned and replaced with new cruelty free platforms that offer reliable and faster results and the ability to carry out personalized experiments.

Organ-on-chip, is a new upcoming technology that utilizes the microfluidic devices and their properties to emulate an organ and it's environment. On these devices, organ-related cells are seeded and nutrients are provided through medium that flows thought the device's channels. An other important aspect of this platform is the ability to emulate a mechanical stimuli that can simulate the organ's mechanical characteristics. Organ-on-chip, is a flexible platform that can be used for drug and therapeutic tests for more precise and personalized results, is cost-effective and can be easily developed.

With that been said, the gut-on-a-chip platform has been developed by researchers and it can enable the further investigation of the gut and it's pathophysiological conditions. For that reason, on this project, we wanted to develop the platform that can be further used for gut-related experiments. Specifically, we had designed and developed the gut-on-a-chip device and enabled the mechanical actuation of the system. The three main components of this system is the microfluidic device, the fluid flow and the actuation mechanism.

In the next chapters, we have described briefly about the gut physiology and the concept of organs-on-chip and then proceeded to explain the method we followed and the way we analyzed our data using microscopy and image processing. Specifically, at the chapter 2 we are looking into the details of gut physiology, the epidemiology of gut cancer and the increasing numbers of early-onset colorectal cancer. Following by the explanation of the gut-on-a-chip concept and the current research on the field. Closing, we have reviewed other organ-on-chip applications.

At the chapter 3, the method we have followed to design and develop the microfluidic device is described in detail. While we also explain, how we have set up the actuation mechanism to simulate the peristaltic-like motion of the gut. Then, the final process to place the components together is described and we present the completed set-up.

Chapter 4, consists of the image analysis and validation method we have followed in order to measure the percentage of expansion of the central channel caused by the mechanical actuation.

On the last chapter, chapter 5 we recap our work and the importance on this project on the endeavors to develop new diagnostic and drug testing tools. Likewise, we express our thoughts and suggestions on what we could done differently and how this project can evolve.

Chapter 2

Literature Review

2.1 Gut physiology

The gastrointestinal (GI) tract, also referred to as the gut, in combination with other accessory organs, form the digestive system, as shown in Fig. 2.1. The digestive system is responsible for breaking the food down, in smaller molecules that can be absorbed and then used by the cells. This process can be split into the following functions: ingestion, digestion, absorption and defecation, different compartments of the GI tract are responsible to carry them out [1].

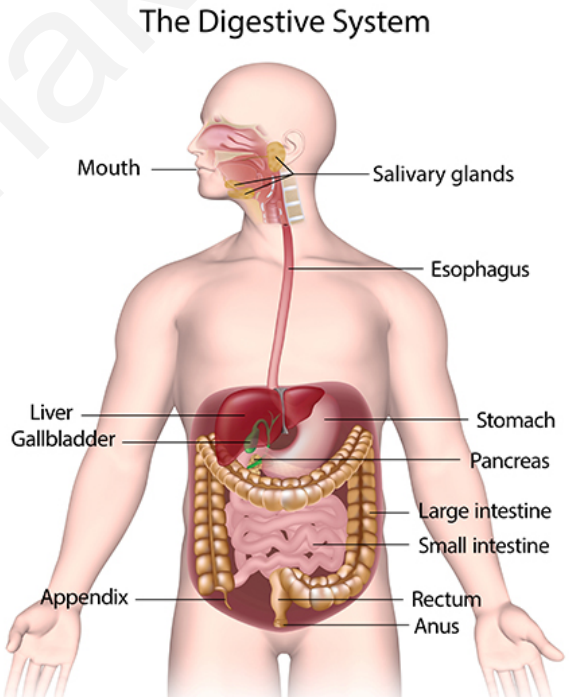

Figure 2.1: Schematic diagram of the digestive system. Image from the article [2]

More specifically, the GI tract consists of the oral cavity, pharynx,esophagus, stomach, small intestine, large intestine and anus. The accessory organs include the teeth, tongue, salivary glands, liver, gallbladder, and pancreas [3].

The walls of the gastrointestinal tract despite the separation in different compartments consist of four tissue layers, starting from lumen: the mucosa, submucosa, muscularis, and serosa as shown in the Fig. 2.2.

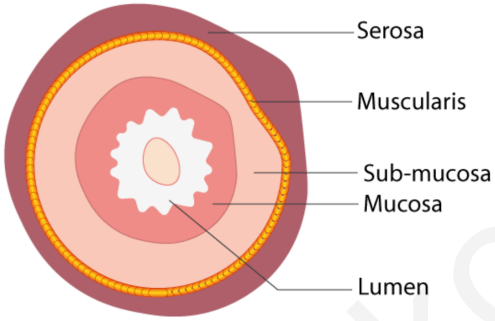

Figure 2.2: GI tract tissue structure. Image from [4]

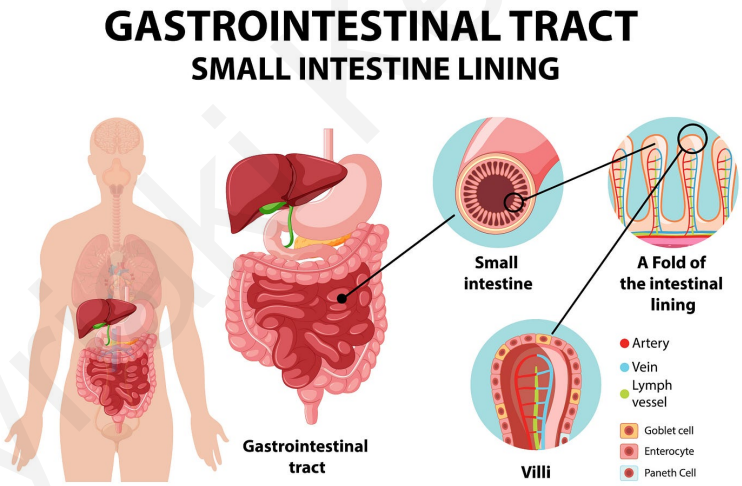

Figure 2.3: GI tract overview. Schematic from [5]

The innermost layer of the mucosa is covered by the epithelium, which directly interacts with the ingested food. The surface of the epithelial cells is increased by the large folds called villi (Fig. 2.3) and invaginations called crypts that can also include glands that secrete mucus or other substances to lubricate the solid food for a better flow and absorption through the tract [1]

The muscularis tissue, consists mainly of smooth muscles of circular and longitudinal layers that regulate the movement of food through the lumen of the GI tract. The circular muscles contract and relax involuntarily in a process called peristalsis which is

illustrated in Fig. 2.4, which begins from the pharynx and ends at the anus. Peristalsis assists the propulsion and the absorption of food in a faster manner. Likewise, the forward and backward motion of the longitudinal muscles called segmental contractions (Fig. 2.5) aim to mix and assist the absorption of the food. [1, 3, 6].

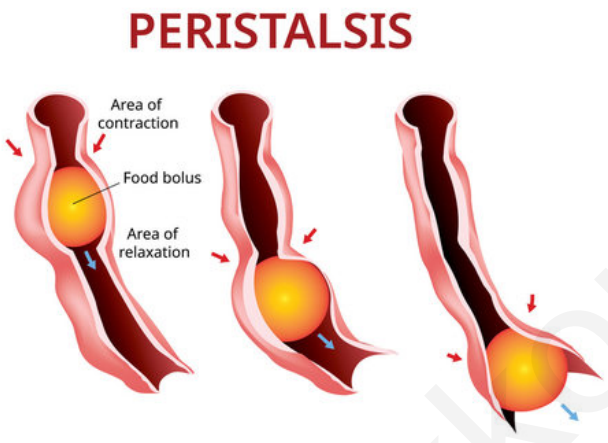

Figure 2.4: Peristaltic motion assist to the faster propagation of the food through the GI tract. Image from [7]

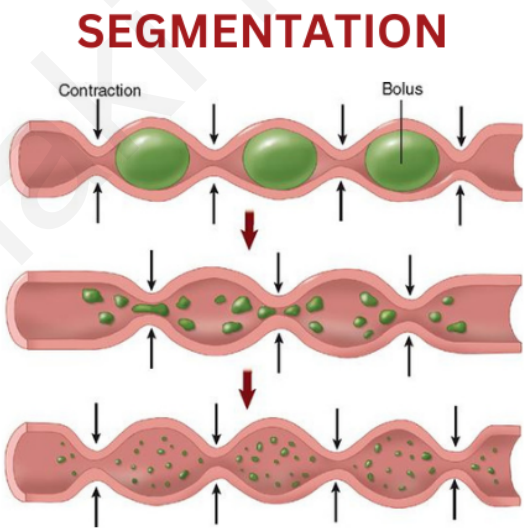

Figure 2.5: Segmental contractions through GI tract lead to segmentation and mixing of food. Image from [8]

Another important characteristic is the presence of microorganisms forming the 'microbiota' in the human gut (Fig.2.6). The microbes and the human have a symbiotic relationship, the first help with the digestion of different substances and the second offers a hosting environment. More precisely, it is estimated that the gut microbiota

is consisted from 10^{14} bacterial cells [9]. The microbiota is a vital part of the gut and assist in the maintenance of homeostasis, absorption of nutrients, regulating the epithelial mucosal barrier and shielding the organism from pathogens. Alterations in the gut microbiome composition can induce pathogenesis [10, 11].

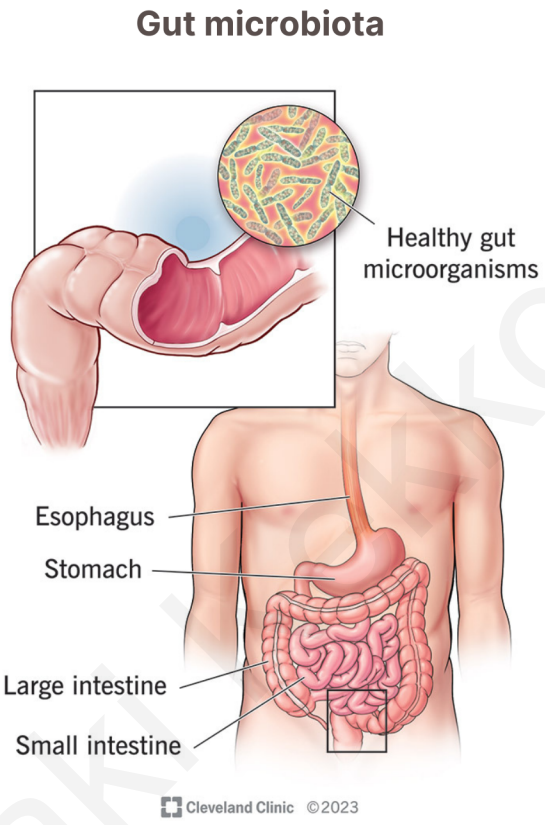

Figure 2.6: Gut microbiota reside in gut of the human body and play a vital role in the proper function of the gut. Image adapted from [12]

2.2 Gut cancer

Gastrointestinal cancer constitutes one of the most common cases of cancers representing a quarter of new cases from all the cancer types. Based on the data from 2018, there were approximately 4.8 million new cases and 3.4 million deaths of GI cancers globally. That translates into 26% of new incidents and 35% of deaths that have been reported from cancer as a leading cause [13].

More specifically, colorectal cancer with 1.8 million new cases comprises the most common cancer of GI tract, followed by cancer of the stomach with 1.0 million cases,

the liver with 840,000 cases, the esophagus with 570,000 cases, and the pancreas with 460,000 additional cases, as they appear in the Fig. 2.7.

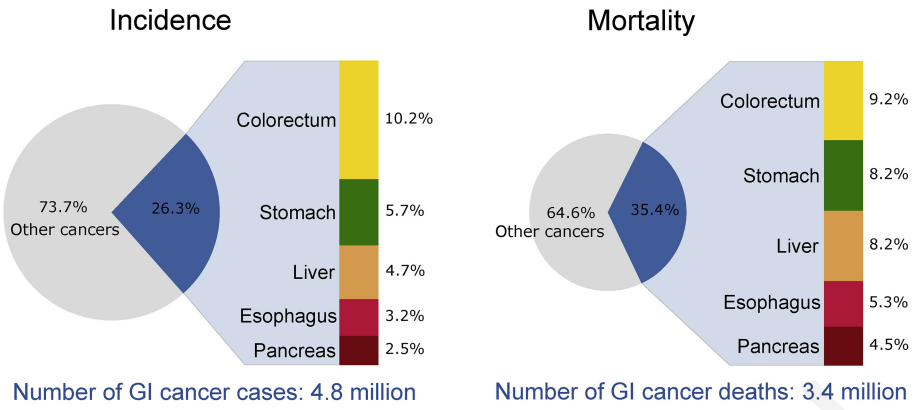

Figure 2.7: The percentages in incidence and mortality of GI tract most common cancers. Image from [13]

In fact, the cancers of the GI tract have some common risk factors but there is a heterogeneity in their epidemiological profile due to the cellular and tissue differences that correspond to the specific organs' micro-environment and functionalities [13, 14].

Cancer has been predominantly associated with aging and since the lifespan of the population has increased, the number of cancer incidents has consequently increased as well. However, current evidence suggests that the prevalence of risk factors has affected the number of incidents and their geographical and temporal appearance, the data are shown in Fig. 2.8 by regions. Particularly, this seems to be a result of socioeconomic changes that are happening globally including the shifts in diet, the increased consumption of processed foods, and the combination of habits that lead to obesity. These factors possibly can lead to various chronic non-communicable conditions (NCDs) and GI cancer [15–21]. Also, common risk factors for most GI cancers include alcohol consumption, smoking, and infections that increase the possibility of developing cancer [13, 22].

Apart from that, the socioeconomic status of people prevents access to healthcare and basic services like vaccination, preventative exams, and diagnostics. Thus, variations through different areas are expected and justified due to health inequality, in addition to the genetic and geographical factors [23].

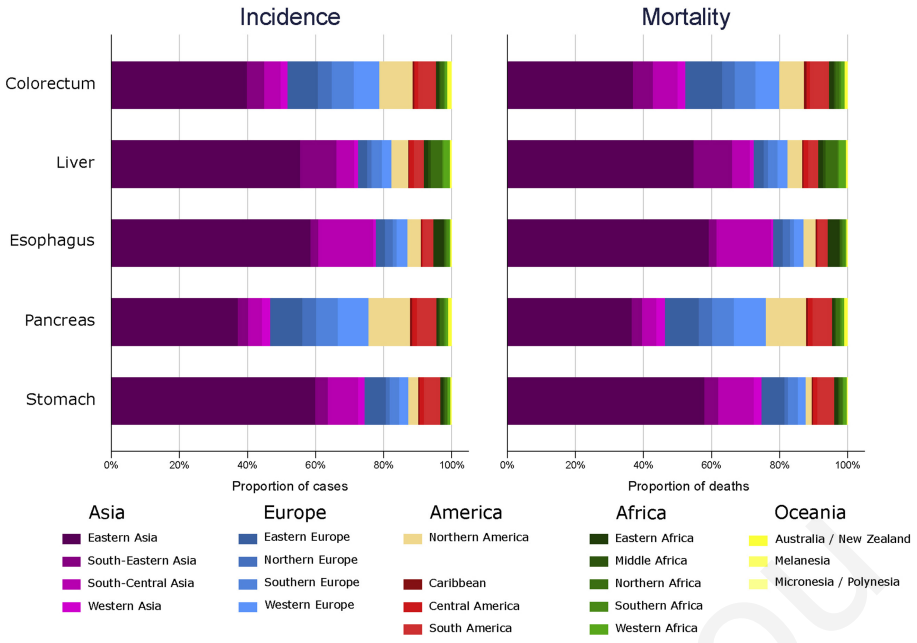

Figure 2.8: Geographic and temporal variations in the incidences and mortality of the different types of GI cancers. In Asia, there were higher rates of liver, esophageal, and stomach cancer whereas in Europe and North America, the main burden was colorectal and pancreatic cancer. Image from [13]

The fact that the population is more susceptible to multiple risk factors shifts the age of diagnosis; younger people are been diagnosed with common cancer types that previously appeared in older people. This phenomenon is described as an early-onset (EO) cancer (Fig. 2.9) and is defined as the cancer that occurs in adults in the age between 18-49 [13, 24].

Global Cancer Observatory (GLOBOCAN) listed the types of cancer with rising incidences including six GI tract-related cancers (colorectum, extrahepatic bile duct, gallbladder, liver, pancreas, and stomach cancer). The research community globally has set as a higher priority the investigation of EO's cancer leading causes which are not clear. GI tract-related cancer, especially early-onset colorectal cancer (EO-CRC), stirs up concerns and the following discussion will focus on colorectal malignancies.

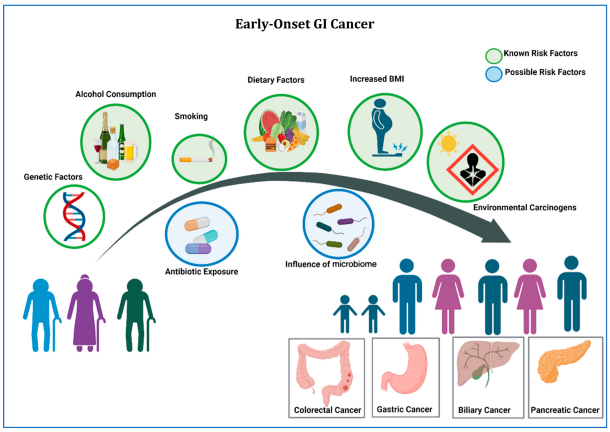

Figure 2.9: Overview of the risk factors for developing cancer in the gastrointestinal system. Age and other mutagenic causes can lead to colorectal, gastric, liver, pancreatic, or esophageal cancer. Image from [25]

2.2.1 Colorectal cancer

Colorectal cancer (CRC) refers to the different types of cancers that appear in the large intestine and they are broadly divided into colon, rectal, and anal cancers. As mentioned above, CRC is the third most common cancer globally [26] and the number of incidents is increasing at an alarming rate, especially in the EO cancer cases. Socioeconomic alterations are directly correlated with the rise of incidence and the risk factors are re-evaluated (Fig. 2.10).

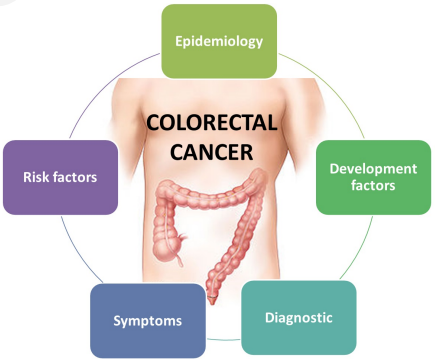

Figure 2.10: Colorectal cancer is the broad term for the cancers that appear in the large intestine. Colorectal cancer's is a multifactorial disease, making it even more difficult to understand the causes and find out the treatment. Source [27]

The incidence of CRC varies across the world with the causes not being totally clear,

more specifically Australia/New Zealand have the highest rate of incidents while South-Central Asia has the lowest. There is a correlation between the high development index (HDI) and the number of incidents of CRC, since countries with high HDI display three times higher rates in comparison with countries having low and medium HDI (2.11). At the same time rising of incidents is detected in countries with low HDI as well, since the combination of healthcare inaccessibility and the occurrences of other risk factors is an issue [13, 14]. The fact that the increase of cases in previously low-incidence regions can be attributed to what we mentioned above, the lifestyle shifts that resulted in higher intake of processed and animal-source foods, especially red meat, the absence of physical activity, and obesity. Likewise, the early exposure to other risk factors led to an emergence of EO-CRC [28–30]. Specifically, the anal cancer has been direct linked with the infection from the human papillomavirus type 16 [31]. Lastly, other lifestyle-related risk factors for CRC are alcohol and smoking [32].

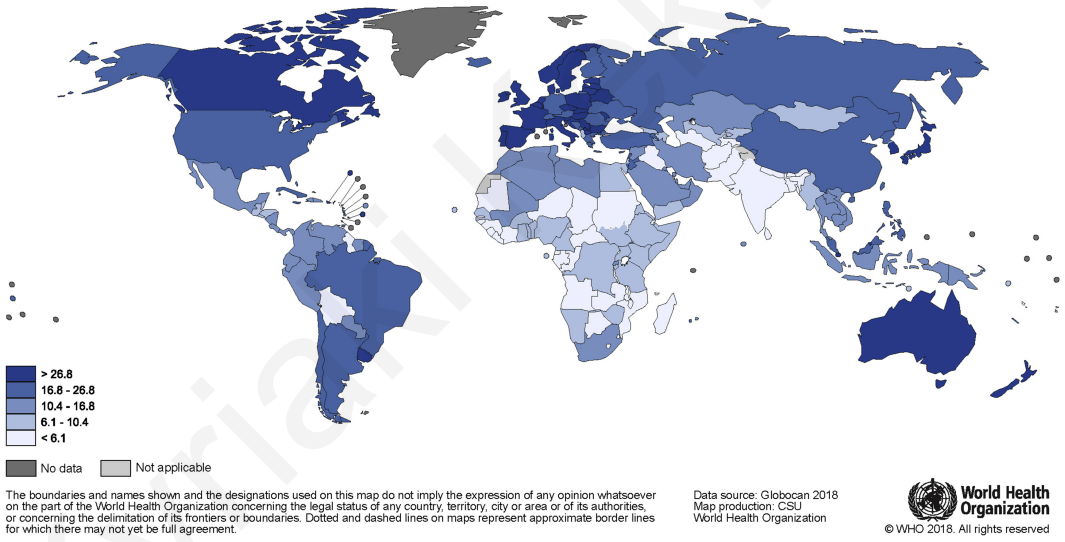

Figure 2.11: Geographical allocation of age-standardized CRC incidents per 100,000 person-year in 2018. Image from [13]

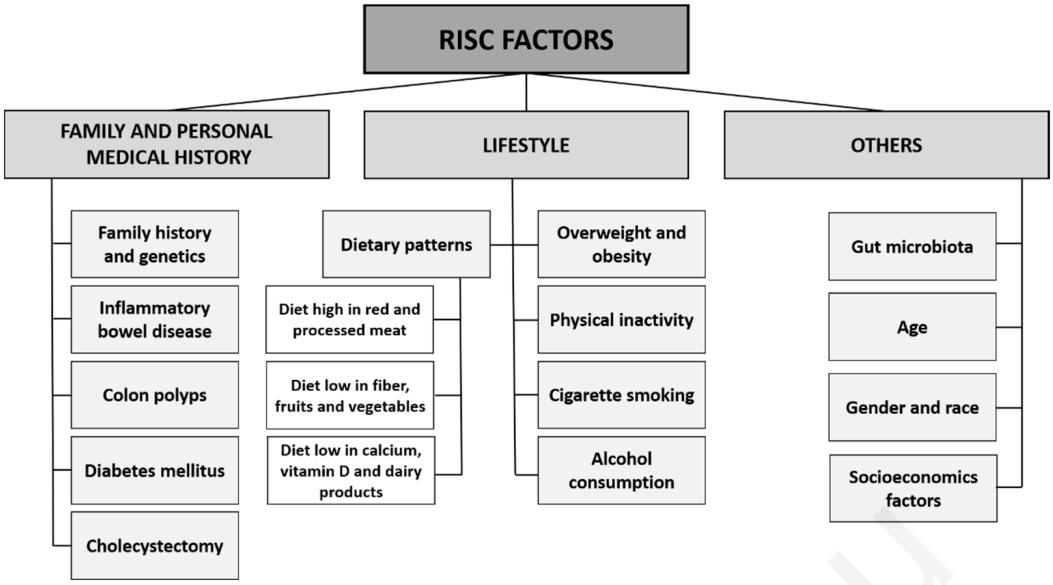

Figure 2.12: Diagram of the risk factors for CRC. Source [27]

Also, the appearance of CRC has been closely related to other environmental and biological factors like the medical history of the family. Statistical evidence has shown that approximately 28% of people with EO-CRC, had a family history with the corresponding kind of cancer [33]. CRC factors are recapped in the diagram Fig. 2.12.

Early detection is a key factor for CRC survival, since the prospects of cure are generally good [34]. Through stool-based tests and endoscopic methods, the precursor lesions can be detected and removed during the endoscopy. [35]. In recent years countries have introduced population-based screening campaigns and the impact soon will be shown in the cancer's stage distribution as well as in the mortality rates [36]. In addition, an important determinant of CRC mortality is the adoption of the best practices to deal with and treat CRC cancer. Considerable advances have been noted in the field of therapeutics and surgical operations reducing the mortality rates. Despite this reduction in mortality rates, the number of CRC incidents in the older population is expected to double by 2035 worldwide due to the increase in life expectancy [37].

2.3 Gut on a chip Concept

In order to deal with the challenges mentioned above, researchers are constantly aiming to improve the detection and prognostic tools, therapeutics, and testing platforms.

An upcoming technology called organ-on-chip enables the imitation of an organ environment in a controlled microfluidic device. The microfluidic device is a very

small elastomeric platform with channels, inside which fluid flow can circulate. For the purposes of an organ-on-chip application, a cell culture is established inside the channels and a nutrient flow is enabled to keep the cells viable. Many times additional parameters are crucial for replicating the micro-environment inside a specific organ, like the lung or gut, requiring breathing or peristaltic motion, respectively. Thus, the addition of more channels in the device enables the application of controlled vacuum that replicates the desired motion. For each organ, the organ specific characteristics are taken into consideration to re-create the environment as faithfully as possible.

In 2010 the first application of lung-on-a-chip was officially published and soon after that the first gut-on-chip application was reported by Kim et al. [38] in 2012. This study presented the first model that supported the culture of Caco-2 cells with living microbiota. In the following sections (Sections 2.3.1, 2.3.2, 2.3.4), we will proceed to give a more detailed description of this pioneering work.

2.3.1 Device fabrication

In this early paper [38], the gut-on-a-chip microfluidic device was fabricated with the use of a flexible polymer called polydimethylsiloxane (PDMS) and consisted of two PDMS layers placed together with a porous membrane in between.

By using soft lithography, the micro-channels were cast on the PDMS layers with the use of a mold with the microchannels design. The PDMS was prepared by using 15:1 of base to curing agent. Respectively, the porous membrane was micro-fabricated by using a silicon wafer with circular post arrays. The membrane was 30 μm thick and had circular porous with 10 μm diameter.

After that, the membrane and the upper layer were exposed to the plasma treatment by the corona treater. Then the membrane was placed on top of the upper layer and like that, they were placed in the incubator for a night at 80°C. The bonded upper layer membrane and the lower layer were exposed to the plasma treatment and then placed together in reverse alignment and left to cure overnight at 80°C.

When the whole setup was fully bonded, blunt needles connected with tubes were placed in the device as shown in Fig. 2.13.b. The tubes in the central micro-channel were placed to control the culture medium flowing through the device. Respectively the tubes in the side chambers were used for the vacuum application controlled by a computer, that emulates the peristaltic motions of the gut, shown in the schematic of

Fig. 2.13.d.

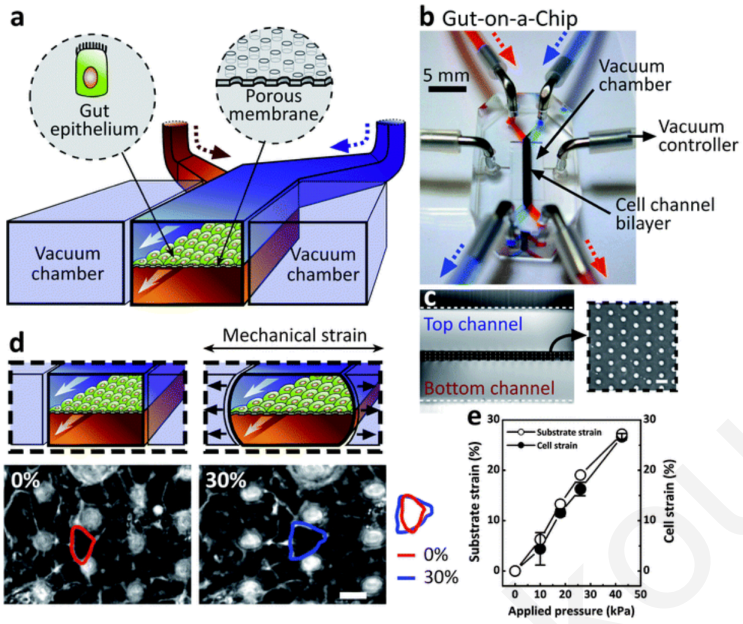

Figure 2.13: Representation of the gut-on-a-chip application source [38]. (a) The microfluidic device for the gut-on-a-chip application presenting the central channel with the porous membrane gut epithelial cells. In both of the sides and the vacuum chambers in both of the sides. (b) Completed gut-on-a-chip device with the tubes attached for enabling fluid flow and vacuum introduction. Blue and red dyes are visible passing through the central channel. (c) Section showing both of the channels and the membrane between. (d) Representation of the difference in the shape of the cells with and without mechanical strain. In the contrast images(bottom) the red and blue outlines specify the shape of the epithelial cells when the expansion of the channel was 30% following the direction of the arrows. The white circles are the porous of the membrane. (e) The diagram quantifies the the strain in both of the porous membrane and the cells, open circles and close circles respectively in response to the vacuum application.

2.3.2 Cell culture

Following the assembly of the device the cultured of the cells was the next step. The human intestinal epithelial cells Caco-2 (Caco-2BBE human colorectal carcinoma line28) were prepared to be cultured in the device. Likewise, the device was prepared to accommodate the cells by ethanol sterilization, and exposure to ultraviolet light and

ozone.

Micro-channels were injected with an extracellular matrix (ECM) containing collagen and Matrigel and then a culture medium was perfused through the device. Then, Caco-2 cells were plated and successfully attached onto the upper surface of the porous membrane within half an hour. Cell adhesion was observed within an hour at which a fluid flow on the upper channel was activated to assist with the development of a monolayer. After a day, the fluid flow was enabled in both channels with a constant flow rate at 30 µL h−1.

To emulate the peristaltic motion of the intestine, a FX5K Tension instrument was used to control the periodic application of a vacuum pressure to the vacuum chambers. The application of vacuum and the cyclic movement caused by it simulates the deformation of the cells in the intestine. A mean epithelial cell strain with 10% expansion and 0.15Hz frequency was successfully emulated during the peristaltic motion of the device.

2.3.3 Study findings

A study to evaluate the differences between the cells in a static Transwell device and a gut-on-a-chip with or without mechanical strain was carried out. It was reported that the growth of epithelial cells took only 3 days but regularly in the Transwell device cell growth takes 3 weeks.

Afterward, further studies with phase contrast and immunofluorescence microscopy showed confluent polygonal epithelial monolayers with well-formed tight junctions. The use of confocal fluorescence microscopy showed that the cells in Transwell were flat and had a squamous form counter to the ones in the microfluidic device with a polarized form and size 6-fold taller.

Fluid flow tests were carried out to evaluate the importance of the rate and the effects on the cells. Thus, fluid flow at 30 µL h^{-1} leads to columnar shaped cells that emulate the healthy epithelial cells and accelerates the cell differentiation within 3 days. In contrast, mechanical motion didn't cause any change in the resulting cells.

In addition, a spontaneous formation of intestinal villi by Caco-2 cells was first reported in this study. After the cells were cultured in the device for longer periods with fluid flow and mechanical strain exhibited a physiological morphology of an intestinal villus as shown in the Fig 2.14. Also, the marker mucin 2 was observed in the apical

surfaces of the villus mimicking the natural deposition.

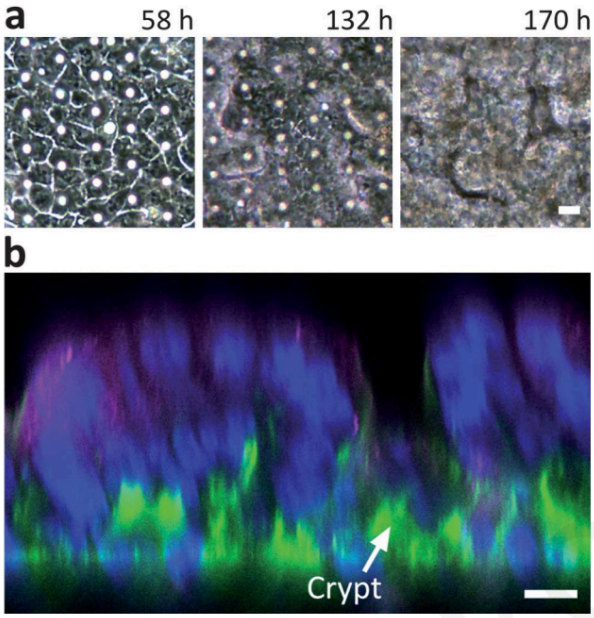

Figure 2.14: ((a)Phase contrast images of the Caco-2 cells were taken during the 58, 123 and 170 hours of culture and the villi formation was visible. Flow and cyclic strain were applied.(b) The confocal fluorescence image at 170 hours, indicates the formation of villi. Where with green stain are the epithelial cells, with blue stain the nucleous of the basal cells and with magenta the mucus. Source [38]

2.3.4 Host-microflora co-culture

The possibility for microbial flora to survive in the device with the Caco-2 cells was studied with the co-culture of the Lactobacillus rhamnosus GG(LGG) in the upper surface of the Caco-2 cells. A continuous flow, 40 µL h−1 and cyclic strain 10%, 0.15 Hz, were applied for 96 hours and resulted in the formation of LGG microcolonies. Staining with calcein-AM and ethidium homodimer-1 confirmed that 95% of the LGG cells remained viable. When LGG is cultured alone, it expresses β-galactosidase activity, that epithelial cells do not express, the activity of β-galactosidase in the device was high justifying the existence of LGG cells. LGG cells that were highly adherent into the epithelial cells remained there and the other ones washed out due to the continuous flow causing no unwanted cultures. After the addition of microbes, the epithelial cells maintained their normal barrier functions, which were even enhanced later, consistent

with the research claims.

2.4 Current Gut on Chip Systems

Kim et al. [38] application is consider the "prototype" for future research in the topic, but other similar approaches have been reported since. In general, based on the application and the study goals, the microfluidic device can differ (Fig 2.15). More specifically, the cells that are used into the microfluidic device can be divided into four categories: the primary cells, the Caco-2 cells, pluripotent stem cells and the adult stem cells. Likewise, the microfluidics can be categorized into mono-environment and multi-environment devices, where the first has more simplified structure and focusing on culturing either endothelial cells or microbiota, while the multi-environment devices are multi-layer structures that support more complex applications [39], like the ones emulate diseases or infections (Fig 2.16, Fig 2.17) .

Further studies have enhanced the knowledge around the intestinal morphology and the microbiota that inhabit it. Aerobic and anaerobic human gut microbiota were co-cultured with epithelial cells in the microfluidic device for a prolonged period. The physiological oxygen gradient was controlled and assessed instantaneously and it was possible to maintain the steep oxygen gradient similar to the intestinal on. These environmental characteristics led to the increase of the intestinal barrier function and to the maintenance of microbial diversity [40].

In another gut-on-a-chip application the role of physical stimulus on the intestinal morphogenesis was investigated, by incorporating mechanical deformation and fluid flow. In the system both Caco-2 and intestinal primary epithelial cells were cultured and formed 3D villi-like morphology that matches the expected 3D epithelial morphology that computational simulations described. This platform is a useful tool for stem cell biology [41].

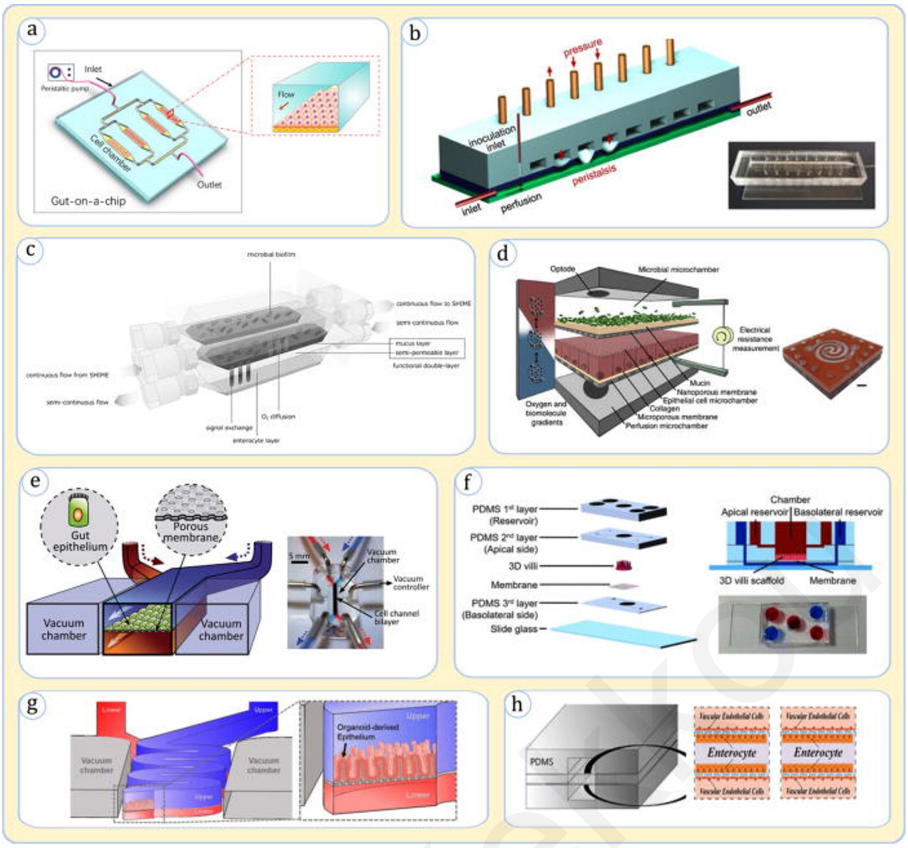

Figure 2.15: Representative applications of gut-on-a-chip, Image from [39]. a) A simple device with microchannels used for culturing intestinal cells. Image source [42] b) A schematic of a minigut device that consist of one channel and supports contractions that mimic the ones of the colonic walls, using membrane deformations along the channel. Image from [43]. c) Device type called HMI (host–microbiota interaction) which consist of two compartments separated by a porous membranes with a mucus layer. In one compartment reside the microbial communities and in the other the entorocytes. Schematic from [44] d) HuMiX (human–microbial crosstalk) that extends the HMI function and incorporates the basal side of epithelial cells as well. From [45] e) The application from Kim et al. [38] that was mention above. In the luminal channel are placed both the enterocytes and the microbiota. f) In this device, a 3D villi collagen scaffold was added. Image from [46] g)This device's luminal and vascular channels have convoluted shape. From [47]. h) In that device there is on luminal central channel with two vascular channels.

In an intestine-on-a-chip application epithelial cells from healthy regions of intestinal biopsies where cultured. The primary epithelial cells were expanded and dissociated forming 3D organoids that mimic the human duodenum in vivo as it was confirmed by a transciptomic analysis. The platform can be a useful tool for further studies of intestine's physiology, infections/diseases and therapeutics [48].

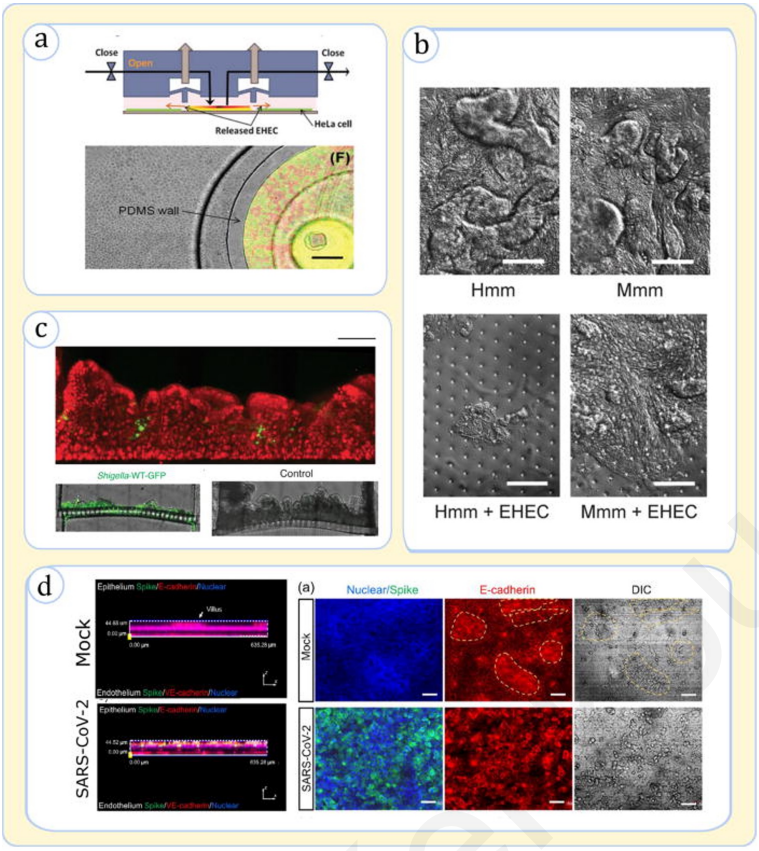

Figure 2.16: Applications that model infections of the gut. Image from [39] a)An application that incorporates HeLa cells with E.coli, in order to simulate the bacterial infection EHEC. Schematic representation of the device (top) and the top view of the device with the EHEC bacteria in red the commensal bacteri in green and the intestinal cells in gray before mixing [49]. b) In another application they studied the damage induced by EHEC infection in human colonic cells in comparison with the mouse that seems more tolerant to infections. The effects of EHEC were studied in the presence of murine (Mmm) and human (Hmm) metabolites. It was found that the presence of Hmm with EHEC leads to a dissolution of the villi in contrast to Mmm [50]. c) The Shigella infection was replicated in another application, and as shown in the top picture, with red is the epithelium and with green are the spots infected with Shigella-WT-GFP. In the bottom images is visible the dissolution of the villi by Shigella-WT-GFP green [51].d) Replication of the SARS-CoV-2 infection in the chip to study the effects in the intestine.As seen in the images the virus causes villi destruction [52].

In a subsequent work by Kim et al. [53], the gut-on-a-chip platform was used for reproduction of the intestinal inflammation by bacterial overgrowth as shown in the Fig. 2.17.a . The model can be used for pathophysiological study and analysis of several diseases that appear in the gut like ileus and the inflammatory bowl disease.

The use of Gut-on-chip system has been extended for a study of the coxsackievirus B1 (CVB1) by replicating and producing the infectious virus in vitro. This virus is related to other health problems like myocarditis, liver and pancreas infection and can lead to severe health issues in newborns [54]. In the application of Villenave et al. [55], the successful use of the model for enterovirus tests was successfully demonstrated.

A Gut-on-chip model was used for testing gamma radiation and its effects to the cells, to replace the murine models [56]. It has been proven that ionizing gamma radiation for therapeutic purposes can lead to different intestinal injuries like hemorrhage, sepsis and subsequently to death [57].

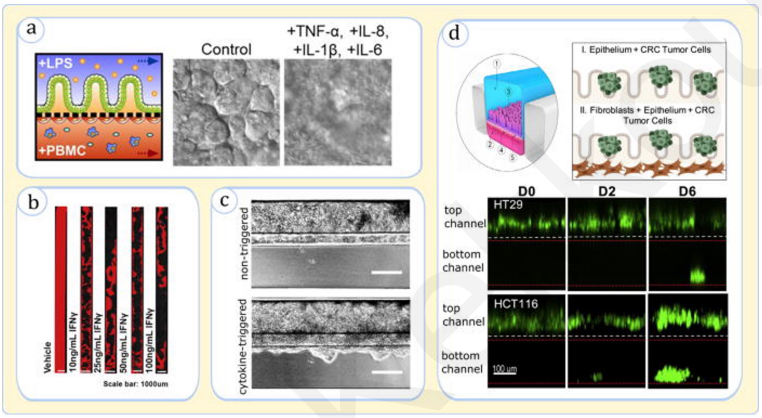

Figure 2.17: Modeling of diseases in the gut-on-a-chip devices. Image from [39]. a) Simulation of inflammatory bowel disease (IBD), with the use of pro-inflammatory cytokines that cause villus injury [53]. b) In an application of colon-on-a-chip, they were studied the effects of barrier disruption. The red staining represents the epithelial cells that are positive to the DAPI(4 ,6-diamidino-2-phenylindole), IFNγ (interferon-γ) a pro-inflammatory cytokine decreases the epithelial layer confluency after 48 hours treatment with different concentrations [58]. c) In another application of IBD study the epithelium was subjected to the effects of cytokite cocktail containing IL-1β, TNF-α, and IFN-γ for eleven days. As shown in the picture the epithelial cells started moving invading the ECM [59]. d) A colorectal cancer was emulated in the microchip environment. The CRC lines HCT116 and HT29 were used and as shown in the figures, both tumors invaded the bottom channel with HTC116 apparently more invasive [60].

2.5 Other organs on chip

The research around the concept of organs-on-chip OOC is continuous and new findings are published often. Thus, in this review we present some of the initial studies and basic concepts for different OOC and how the science has exploited their capabilities.

2.5.1 Liver on a chip

Liver is a vital organ with high metabolic activity, since it's responsible for metabolizing nutrients, detoxifying blood and producing molecules important for digestion. Due to their high activity, hepatic tissues are highly regenerative and complex hepatic lobules are formed in the liver that contribute to the multicellular communication and completion of hepatic functions [61]. A platform mimicking the liver is highly needed, since many drug trials fail due to liver toxicity [62].

In the first liver platform Kane et al. [63] cultured 3T3-J2 fibroblasts and rat liver cells where the hepatocytes could carry on the metabolism process and synthesize albumin. Lee et al. [64] introduced a chip that mimicked the liver sinusoid structure by placing endothelial cells and hepatocytes into a microchannel with a culture medium circulating through the system. Transport phenomena were observed in the sinusoid area by the endothelial cells which enabled the exchange of substances. Likewise, in the work of Delalat et al, [65] where screenings where carried out to evaluate new drug toxicity. An integration of a sensor with the liver-on-chip has also been be seen [66] which could track the glucose and lactate concentrations. The data from the metabolic activity could give insights about response to the mitochondrial dysfunction. Kamei et al. [67] used a microfluidic platform for maturing hepatocyte-like cells that differentiated from human pluripotent stem cells(hPSCs).

The effort to construct 3D structures in the platform was also studied. Lee et al. [68] developed a platform that accommodated monocultures and cocultures of hepatocytes and hepatic stellate cells which formed 3D structures. Then they were able to investigate the interactions between these cells with or without flow, that could managed by an osmotic pump. Hepatic lobule structures where firstly grew by Ho et al. [69] using dielectrophoresis (DEP) to pattern the cells into the microfluidic platform. Different techniques were derived to improve the physiological conditions and lead to a better recapitulation of the liver 3D model [70], [71], [72]. Likewise, to evaluate the cytotoxicity in other cells but also identify biomakers that might be produced during toxic

reactions, [73, 74]

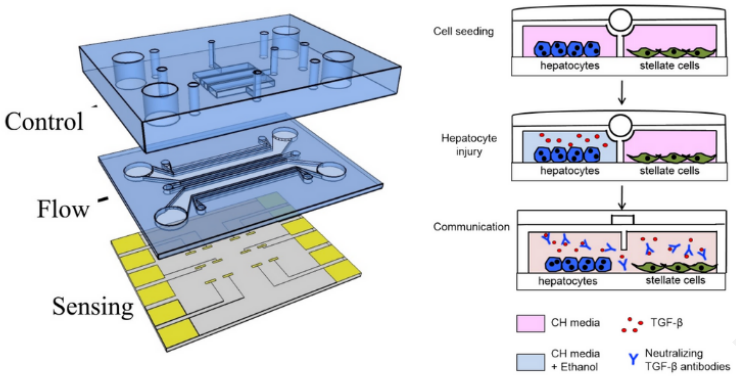

Figure 2.18: On the left side is the liver-on-chip platform integrated with a sensor. On the right side is a schematic representation from the beginning of cell seeding, the administration of the alcohol and the effects of it. The study found that alcohol causes the hepatic cells to secrete TGF-β molecules, that are transferred, to the near by stellate cells causing them to produce more TGF-β. Image from [75].

In order to recapitulate different reactions and injuries of the liver multiple applications were developed. One of these platforms,could be used as tool to identify substances that caused systematic skin reaction [76] based on the different metabolic derivatives. A hepatitis B virus was also replicated and investigated [77] in a microfluidic platform. Injuries and other effects caused by alcohol were investigated through metabolomics, proteomicss, genomics and epigenomics [75] (Fig 2.18).

2.5.2 Lungs on a chip

In the respiratory system the exchange of gases between the blood and the air takes place; this process is regulated by lung's alveoli. Breathing is accomplished through the mechanical motion that happens periodically and is difficult to be replicated in vitro. Thus, lung-on-a-chip offers the ability to replicate the motion and the physiology of a real lung. The device can enhance the search to investigate further the lungs and the related diseases, but also act as a platform to test drugs.

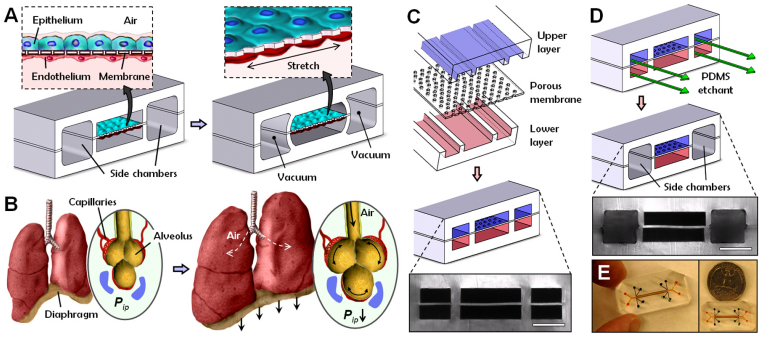

Figure 2.19: Schematic representation of the lung-on-a-chip device and the parts consisting it. A)The platforms mimics the alveolar-capillary barrier with the use of porous membrane and the breathing motion by applying vacuum at the vacuum chambers. B) The contraction of the diaphragm during inhalation leads to the reduction of the intrapleural pressure - Pip and to the distension of the alveolar-capillary interface. C) The placement of the PDMS layers. D) The two side chambers are created by the selective etching of the membrane layers. E)Lung-on-a-chip microfluidic device. Image from [78].

Huh et al. [78] developed the first biomimetic microsystem of lung-on-a-chip (Fig. 2.19) which reconstitute the critical part of a lung the alveolar-capillary interface. This model actually was mimicking the breath by recapitulating the important characteristics of the lung, including the structure, the functionality and the mechanical properties of it. They used soft lithography to reproduce the chip's channels of both of the PDMS layers. In the upper PDMS layer there were cultured alveolar epithelial cells and in the bottom, human pulmonary microvascular endothelial cells that were separated by a porous membrane (10 μm) that acts like an interface between the two. A lateral vacuum was applied to simulate the expansion and contraction of the human lungs during breathing and it was found that it indeed affected the experimental data. Through this system they were able to test the processes and responses to infections and nanoparticles.

Stucki et al. [79] reported a system that mimics the lung parenchyma that includes the alveolar barrier. The main objective in this work was to grow the bronchial epithelial and endothelial cells under a cyclic motion that mimics the respiratory one and study how this motion affects the epithelial barrier permeability. In addition to that,

through this study they observed an improvement in the cell cultured in comparison to the static ones.

Humayun et al. [80] incorporate a hydrogel micro-layer in the lung-on-a-chip device and then cultured airway epithelial and smooth muscle cells to study if they are suitable model. The combination of collagen Type-1 and Martigel showed better results to the cell adhesion in the device and the group was able to use it as a tool to evaluate chronic lung diseases. In a different application Yang et al. [81] used a poly(lactic-co-glycolic acid) electrospinning nanofiber membrane as a chip matrix for cell scaffolds into the lung-on-a-chip device. In that way enables the device to be used as a tool for tissue engineering but also as tool for tumor precision therapy.

Jain et al. [82] set up a therapeutic model for intravascular thrombosis that appears in the lung alveolus. The importance of that project lies to the fact that, they are able to test different drugs like the antagonist to protease-activated receptor-1 indicating that it can be used as a platform to develop and test antithrombotic drugs. In the work of Si et al. [83] they investigate the possibility to replicate the physiology and the pathophysiology of a human lung by developing a lung-airway platform. In the chip were cultured human lung airway epithelial cells and pulmonary microvascular endothelial cells. They studied seven anti-viral therapeutics and demonstrated that the platform can reliably be used to replicate the respiratory diseases.

Umbilical vessel damage by catheters was successfully studied for the first [84], by developing a lung assist device during respiratory failure in a preterm infants. This device improves the gas exchange on the placenta by increasing the diameter of channels in the umbilical arteries and veins and consequently increasing the blood flow. The importance of that project lies in the fact that umbilical vasodilation trials are not ethical. In a similar application [85] a microfluidic lung assist device, acts as artificial placenta type oxygenator using a double-sided gas delivery that improves the oxygen uptake. The double-sided single oxygenator unit (dsSOUs) had increased oxygen uptake up to 343% in comparison to the single-sided SOU (ssSOU).

Benam et al. [86] have developed an "airway-on-a-chip" studying the airways after a chronic asthma and obstructive pulmonary disease and the responses after therapeutics. They also tested the responses of the model to the therapy. The SARS-CoV-2 in 2019 and the unexpected consequences in human health has highlighted the need for a platform to carry out test fast and reliably. In this review [87] were suggested some possible uses of a lung-on-a-chip platform for replicating respiratory diseases and test

drugs.

2.5.3 Kidney on a chip

The kidney is an organ with a sophisticated structure comprising of several types of cells. These cells are distinct into glomerular cells, proximal tubule cells, a loop of Henle cells, thick ascending limb cells, distal tubule cells, collecting duct cells, interstitial kidney cells, and renal endothelial cells [88] . The organ carries on, the filtration of blood by removing the waste and extra fluid from the blood, also helps to keep the balance of different substances in the blood. In the kidney's nephrons take place the process of filtration and re-absorption. Thus, in case of kidney toxicity the issue of losing the renal filtration is major. Finally, the most common impact of a drug is the toxicity of kidney. [89]

Jang et al. [90] was one of the firsts that developed a multi-layered system of a kidney. In that system they added collecting duct cells from mouse to study the filtration process of the kidney. Through this platform the polarity of the inner medullary collecting duct was improved in response to the hormone stimulation. In a similar work, the first model developed for kidney toxicity on primary kidney proximal tubular epithelial cells was developed [91]. The device emulated the fluid perfusion of the human kidney proximal tubule and they were able to study the kidney functions like the absorption of glucose the transportation of albumin and the activity of alkaline phosphatase(ALP).

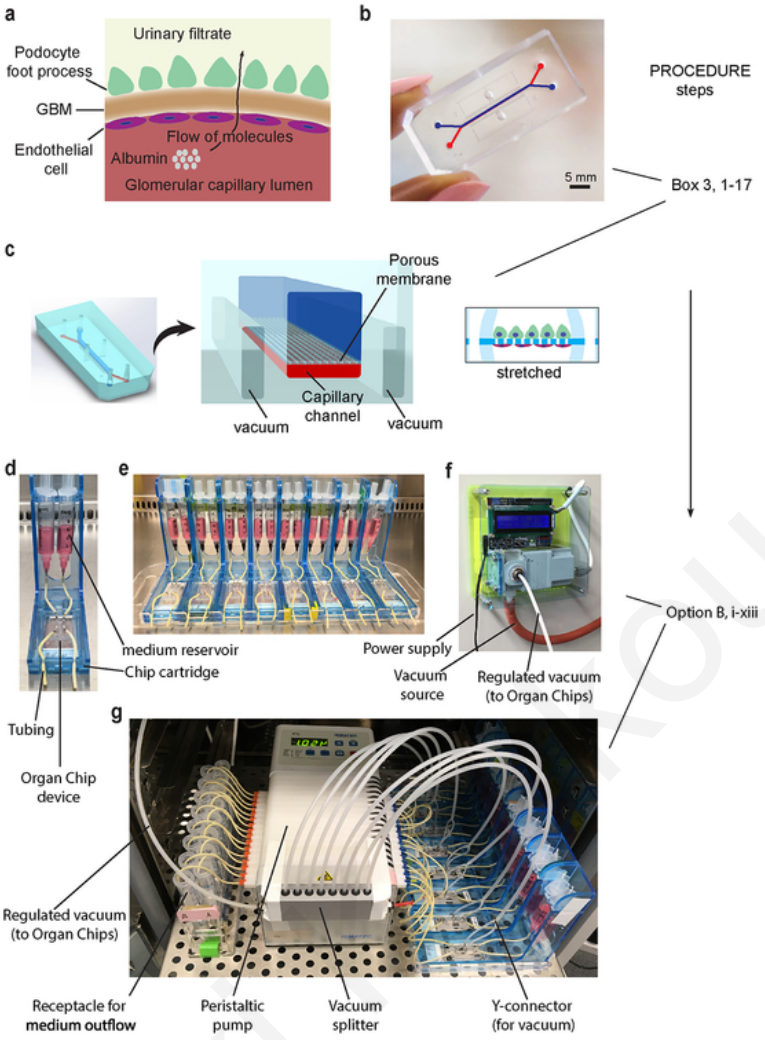

Figure 2.20: Replication of the glomerular capillary wall in a kidney-on-a-chip application. a) Glomerular capillary wall, with podocytes and endothelial cells separated by glomerular basement membrane (GBM). b) Kidney-on-a-chip device. c) The porous membrane functionalized by laminin protein is acting as the GBM. In order to replicate the stretching and relaxation motion observed in living glomeruli a mechanical strain is applied using vacuum. d)The device connected with two reservoirs with cell culture media. e) Multiple devices. f) Vacuum system regulated by a program. g) Complete set-up. Image from [92].

In the study by Wilmer et al. [93] the main aspect was to develop kidney-on-a-chip platform were the characteristics of kidney could be replicated in order to improve the prediction of drug-induced kidney injury (DIKI). Zhou et al. [94] developed a glomerulus-on-a-chip device where they replicated the interface between the podocytes

and endothelial cells in the glomerulus. A key aspect of the system was to apply a fluid flow and mechanical forces, with that they pointed out that shear stress and hydrodynamic pressure leads to cellular cytoskeletal rearrangement and cellular damage.

Musah et al. [95] developed a kidney-glomerulus-on-a-chip where human induced pluripotent stem (hiPS) cells were cultured and differentiated into podocytes. Since the glomerulus has a critical function for blood filtration, podocytes have a key role, that of the permeability regulation. Thus, they created glomerular basement-membrane collage to replicate the tissue-tissue interaction with the glomerular endothelial cells. They were able to replicate the adriamicyn-induced albuminuria and podocyte injury. In another platform they generated human islet organoids from human induced pluripotent stem cells [96]. This presents a new way of engineering organs from stem cells and enables the regenerative medicine. In another application [92] (Fig. 2.20) it was described a method to reproduce pluripotent stem cell-derived podocytes in order to replicate the function and structure of human glomerular on a chip. With the use of the chip they were able to study further the kidney and its diseases but also the nephrotoxicity, therapeutics and regenerative medicines. A three-layer microfluidic platform for kidney diseases caused by virus was developed [97]. The platform mimicked the distal-tubule through which they studied the renal dysfunction in the regulation of electrolyte after virus infection.

2.5.4 Heart on a chip

Heart is one of the most vital organs as it is responsible for the circulation of blood through the body, and cardiovascular diseases are the number one cause of death. Microfluidic-based models of the heart enable further studies in its function and heart related diseases [98].

In one of the first studies around the topic Grosberg et al. [99] developed muscle membranes from a PDMS film and neonatal rat cardiac myocytes cultured on in. Their aim was to measure and analyze the contractile capacity of the myocytes by taking advantage of the membrane curl during contractions. Thereafter, Zhang et al. [100] managed to produced self-assembled myocardial sheets by utilizing hydrogels. In another study [101] micro-organ tissue chips were developed my using a 3D bioprinter. The endothelial cells were produced by the printer and cardiomyocytes were seeded in order to form a vascular network.

The heart-on-a-chip device was introduced by Zhang et al. [102] for detecting the contractions and effects in cardiomyocytes from drugs. The platform was used for preclinical assessments of drugs. Marsano et al. [103] fabricated a heart-on-a-chip microfluidic device that mimicked the physiological and mechanical characteristics of cardiomyocytes(CMs) and could support the beating of them. The mechanical and electrical stimuli that was applied resulted to a better cell coupling. Several concentrations of isoprenaline were tested proving that the device can be used for drug and toxicological tests. Thus, the platform enabled the direct visualization and quantitative analysis that was not possible to the traditional models.

The ability to generate heart tissues from differentiated pluripotent stem cells in a chip, was enabled by the study of Schneider et al. [104]. The platform could preserve myocardial cells for extended period of times without them losing their functional characteristics. Spatiotemporal pulsation dynamics could be visualized through the platform. Similarly, Tzatzalos et al. [105] in the study describes the importance of human induced pluripotent stem cell-derived cardiomyocytes (hiPSC-CMs) in the drug research for cardiomyocytes related diseases. Cardiotoxicity is one of the main factors for drug failure during trials and there is a necessity for reliable test platforms.

In a different application [106], gelatin was used as an extracellular matrix with titanium oxide and silver nanoparticles for the development of mussel-inspired 3D device. The aim of that chip was to test the contractility of myocardial cells after the exposure to nanoparticles that cause toxicity by affecting the calcium signals. Kamei et al. [107] focus was to recapitulate the side effects of doxorubicin (DXR) anti-cancer drug, in an Integrated Heart/Cancer on a Chip (iHCC). The human heart cells (hCMs) and liver cancer cells(HepsG2) were cultured in the device, leading to the production of the toxic doxorubicinol (DXRol) by HepsG2 after metabolizing the drug doxorubicin. The circulation of DXRol in the device caused the toxicity to the heart cells.

2.5.5 Brain on a chip

Brain is consider the most vital organ in the human body since it orchestrates and manages the rest of the body by signals through the nervous system. The fact that the human brain in terms of genetics and functionality is pretty different from the other animals sets limitations to our understanding of it. Animal tests provide only the basic information, but there is a need to find out more about the degenerative diseases and

be able to test the therapeutics.

In one of the first applications [108], in the field on brain-on-chip, a microfluidic device was created to replicate the axonal transport process. The platform enabled the growth of an axon and axonal mitochondria. In the study of Kunze et al. [109], the platform supported the growth of neural layers into 3D structures. The layers were developed by mixtures of agarose-alginate and then cortical neurons were integrated into the system. B27 supplements enabled the formation of concentration gradients in the system. Park et al. [110] presented a microfluidic device (Fig. 2.21) in which sealed microgrooves divide the soma part of the neuron from the axon. This arrangement aimed to physically guide the growth direction of axons. An image processing algorithm was developed that could quantifies the growth of axons. They also investigated the effects of different bio-molecules in the axonal growth.

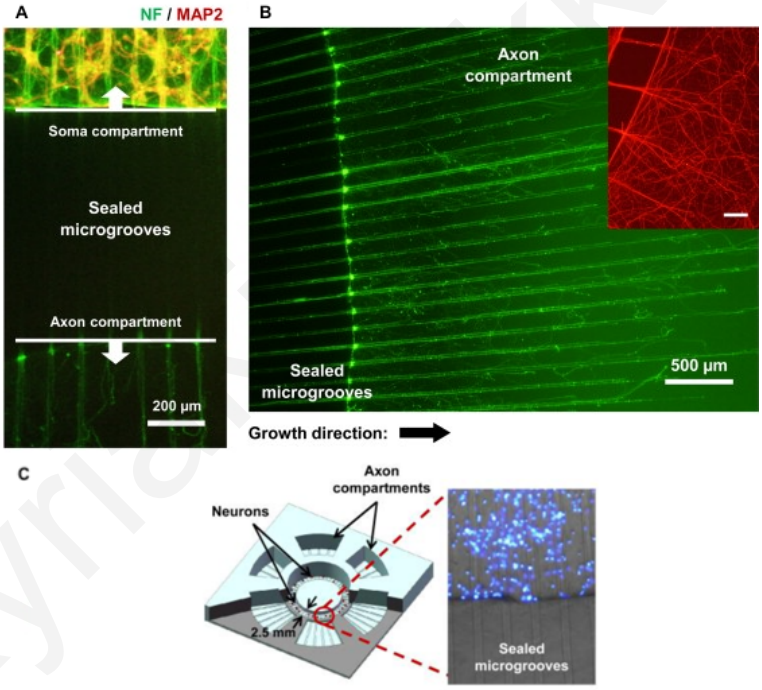

Figure 2.21: a) Schematic representation of how the sealed microgrooves where placed to compartmentalize the dendrites from the axon. NF- green dye is the axon and with MAP2- red dye is the dendrites. b) The sealed microgrooves are guiding the growth of axons in the axon compartment. The inset image shows the growth morphology of the axons without the help of the guiding microgrooves, that leads to difficulties in the analysis of the axons. c)Schematic representation of the device, with visible the compartmentalization of the somata and the axons. In the zoomed in image are shown the DAPI stained neurons. Image from [110].

In an another brain-on-a-chip model by Kilic et al. [111], the growth of neurospheroids was investigated under different environmental factors. By changing the fluid flow, neural networks were created and the occurrence of neural differentiation was observed. The dynamic environment seems to be favorable for neurospheroid's development. Amyloid- effects and treatment with and without flow were also studied. A multi-regional brain-on-a-chip [112] was fabricated in order to investigate different diseases. It was found that the firing activity between the neuronal network was decreased in specific brain regions. The effects of the drug phencyclidine were also reviewed.

Mimani et al. [113] developed a brain tumor-on-a-chip model to study the magnetic hyperthermia, a cancer treatment that aims to protect the cells near the cancer area by generating heat locally. Gliobastoma was cultured on the microfluidic and magnetic hyperthermia therapy was carried out for 30 minutes leading to 100% decrease of the cell viability.

2.5.6 Human on a chip

Human-on-a-chip is the integration of two or multiple organs into one platform with the need of continuous circulation of media and interactions between the different tissues. Human-on-chip which is also referred as a "multi-organ-on-a-chip" [114] can be used for complex studies like drug testing, cytotoxicity [115] with a promise to replace animal tests.

The challenges that need to be addressed for the successful development of that platforms is the production of media suitable for all the tissue types that will not lead to toxic reactions, the proper scaling of organs, the vascularization of tissues and the integration of the immune components. Likewise, the sourcing of pluripotent stem cells (iPSCs) and different biological cell's cycles like the circadian need to be taken into account.

In addition to that, there are some technical challenges that need to be considered in the integration of the multiple organs like the maintenance of sterility in the system and the formation of bubbles during the circulation. Optimizing the physiological parameters of the different tissues and organs like the flow rate, the ideal oxygenation and nutrients level.

In a review [116] the critical parameters of human physiology have been established

along with the limitations based on parametric equations. This review focused on the design of a physiologically based pharmacokinetic (PBPK) and pharmacodynamics (PD) model for drug development. In a multi-organ-on-a-chip model [117] different cells types were cultured simultaneously and were connected by a channel, acting like a bionic blood vessel.

An approach that will eventually lead to a whole human-on-a-chip, is to incorporate few organs each time. Such as the pairs, liver-fibroblast, gut-liver and liver-pancreas. Also the fact that organs communicate through secretion of chemical factors and vesicles should be considered during the integration [118].

The study of metabolism and effects of drugs has enabled the liver-kidney model [119]. In which HepG2/C3A cells were co-cultured with kidney cells to investigate the metabolic changes after drug delivery. In another model of liver-kidney chip by Choucha-Snouber et al. [120] the anticancer agent Ifosfamide was administrated in order to investigate the toxic effects. The results compared with the ones from mono-cultured chip highlighted the importance of multi-organ platforms.

The first interaction of liver and intestine in a microfluidic was presented by Van et al. [121]. The study focused on the interactions between the tissue slices from the two organs in response to metabolization of drugs. The interaction of intestinal and liver slices were demonstrated on this paper by the successful regulation of primary bile acid in the chip. In another application that emulates the liver-intestine-on-a-chip Bricks et al. [122] cultured HepG2 C3A and intestinal Caco-2 TC7 cell lines to investigate the absorption and metabolization of drugs from intestine and liver respectively. The study highlights the importance of intestine in the utilization of oral medications but also the improvement of the experiment's results compared to the ones from the petri dishes.

Maschmeyer et al. presented an application of liver-intestine and liver-skin co-culture models [123] that emulate the toxicity caused by the drug Troglitazone. This anti-diabetic drug was withdrawn from the market since it led to hepatotoxicity.

Vunjak-Novakovic et al. [124] integrated liver, heart and vascular system into one microfluidic. The blood and the corresponding organ cells were cultured into the device which was used as a platform for studying the human physiology in real time.

A four-organ-chip model by Maschemeyer et al. [125] was developed to study the absorption, distribution, metabolism and excretion (ADME) through the co-cultured of intestine, liver, skin and kidney. The platform emulated successfully the physiological

path of a drug delivery in the human body with the discrete physiological functions of each organ. The metabolization from the liver into the metabolization and absorption from the small intestine to the excretion through the kidney with high cell viability the platform offers the ability to evaluate the pharmatokinetics and pharmacodynamics.

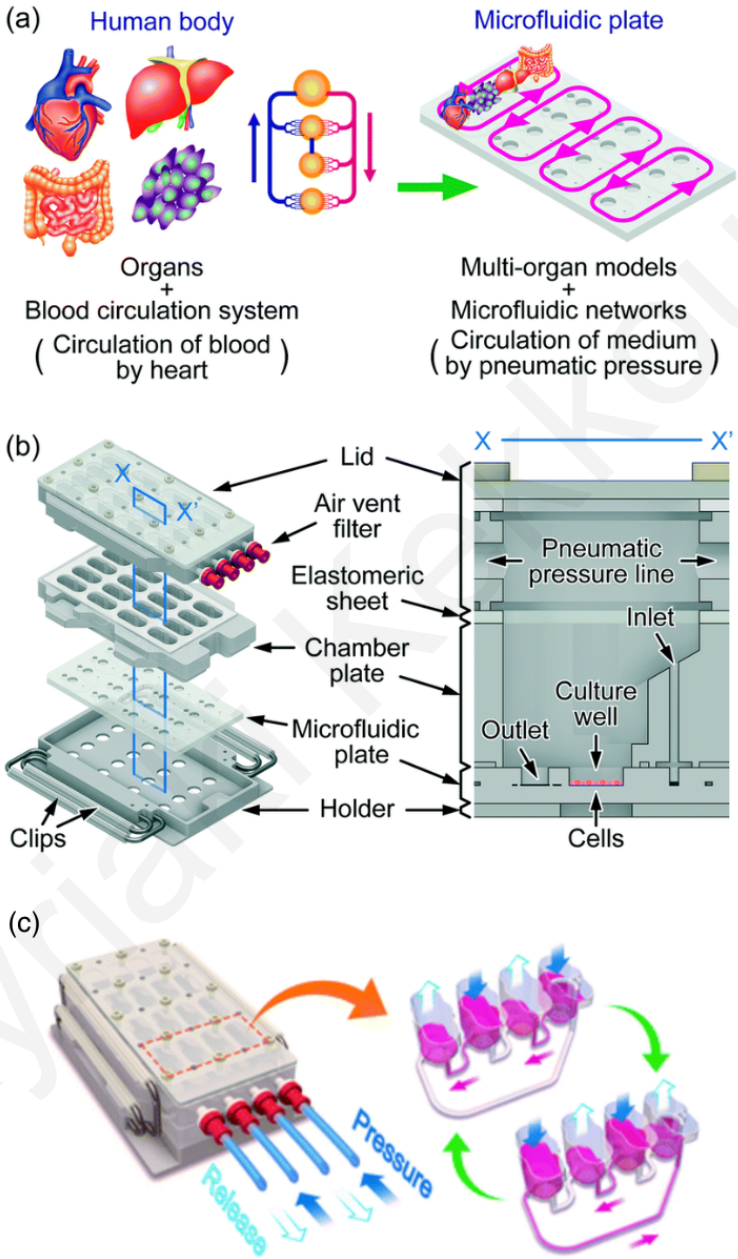

Figure 2.22: The multi-throughput multi-organ-on-a-chip system. Image adapted from [126]. a) This is the idea of how the human body can be replicated into a microfluidic system. b) Detailed view of the device components, with 4x4 culture chambers. c) The schematic representation of how the pneumatic pressure is circulatic the medium through the platform

Satoh et al. [126] developed a pneumatic pressure-driven system that supports simultaneous multiple cultures with multi-inputs (Fig. 2.22). This multi-organ-on-a-chip platform offers flexible design and development of different microfluidic networks, with the ability to handle the liquid flow using the pipette interface. A liver-cancer model was replicated in order to investigate the effects of the anticancer drug capecitabine (CAP) which inhibited the multiplication of the HCT-116 cancer cells. Likewise, in another four-organ model of intestine, liver, cancer and connective tissues the effects 5-FU, CAP and tegafur were evaluated.

The research in the field of human-on-chip is ongoing and new techniques are presented to improve the microfluidics, the control over the cells and the culture conditions [127–130].

Chapter 3

Design and Fabrication

As we have mention in the literature review (Section 2.3), the gut-on-a-chip model constitutes by the microfluidic device that accommodates the gut's cells, the vacuum that enables the emulation of the peristaltic-like motion and a fluid flow system that delivers nutrients and other substances to the cells. In this chapter, we described the process we followed in order to develop and validate the actuation and the control system for the gut-on-a-chip device. The paper from Kim et al. [38] described in the Section 2.3, sparked our interest in the field and acted as the guidance to our efforts.

3.1 System overview

The gut-on-a-chip system is formed by three components, the microfluidic device, the actuation mechanism and the fluid flow mechanism. In order for cells to be cultured into the device, it needs to be placed inside an incubator for maintaining the cells viability as shown in the Fig. 3.1 that represents a completely functional system.

The microfluidic device is the platform where the gut epithelial cells are cultured and supplied with nutrients that flow through its channel. For the purposes of this project, the device is a two layer structure, with a semipermeable porous membrane between the two layers. The membrane act as the interface for the cells seeding and also enables the exchange of substances (nutrients and waste) between the cells and their environment.

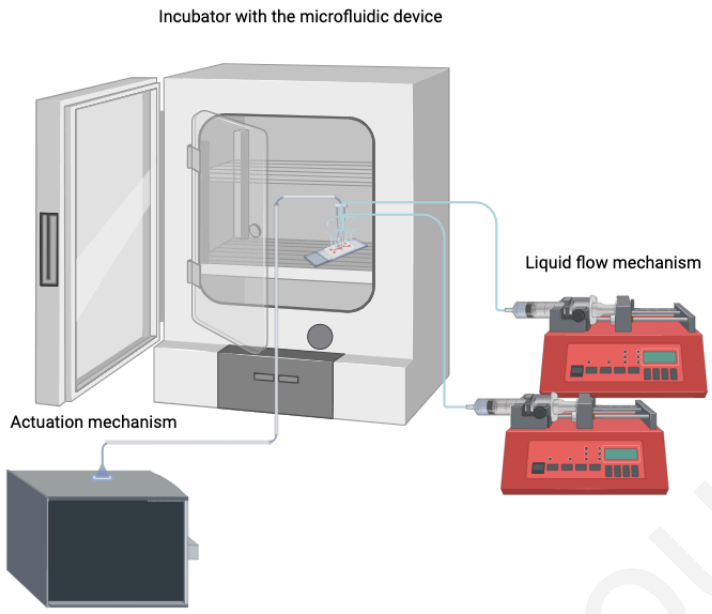

Figure 3.1: This image, shows the gut-on-a-chip full set up. The microfluidic device with the cell culture should be placed in the incubator for the cell preservation. The device is connected with the liquid flow and actuation mechanism, where the first provides the nutrients to the cells while it removes the waste and the second enables the peristaltic-like movement.

This device has one central channel and two vacuum chambers on either side. The two side chambers accommodate the application of the vacuum. More specifically, by applying vacuum in the side chambers, the walls of the central channel are pulled and therefore both the channel and the membrane are expanded. When the vacuum application is terminated the walls return to their initial state. The alternation between vacuum and no-vacuum, in predetermined intervals, resembles the peristaltic motion of the GI walls. As mention in the literature review, the peristaltic motion is an important aspect for the growth and shape of the gut cells.

Lastly, the liquid flow mechanism is responsible for providing and controlling the medium that pass through the central channel of the device. In this microfluidic device, there are two inlets and two outlets and the medium chosen each time is selected based on the requirements of each project and experiment. The schematic Fig. 3.2 shows the device and the flow of mediums through it.

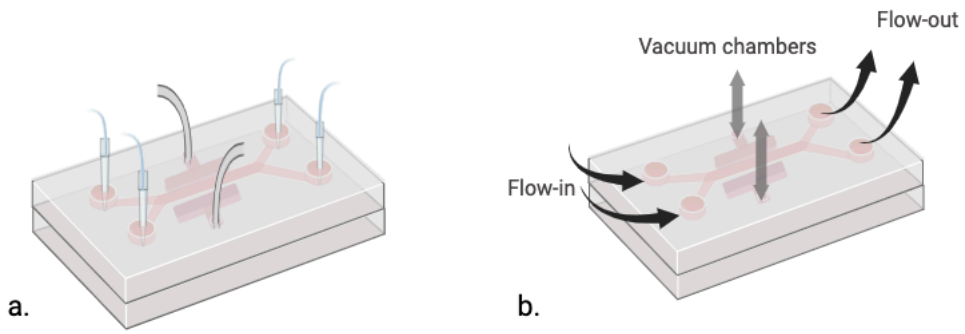

Figure 3.2: a. The microfluidic device representation with the liquid and gas tubes. b. Representation of the liquid/vacuum flow inside the microfluidic device.

3.2 Design

The two layers of the microfluidic device have exactly the same structure and they are produced using the polymer Polydimethylsiloxane (PDMS). The structure consists of one central channel and two vacuum chambers on either side of it, as shown in the Fig. 3.3.

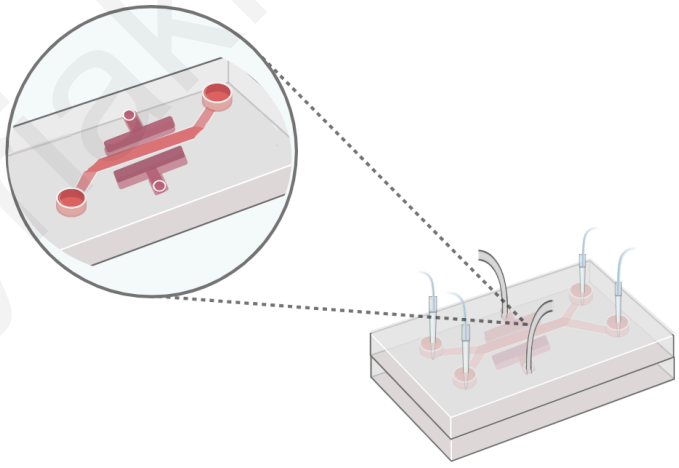

Figure 3.3: The inset image shows the design that is fabricated on the PMDS. We can see that the design consist of the central channel with the two vacuum chambers on each side.

In order to replicate the design on the PDMS, we carried out the soft lithography technique using a mold (the soft lithography technique is described in details at the Section 3.4). The mold was also designed and produced using the 3D printing. For

that purposed we used a 3D design tool called Tinkercad that provides the interface to create 3D objects and visualize how they will look like when printed. Thus, we designed the structure for a single layer and duplicated it on a slab creating four pairs as shown in the Fig. 3.4.

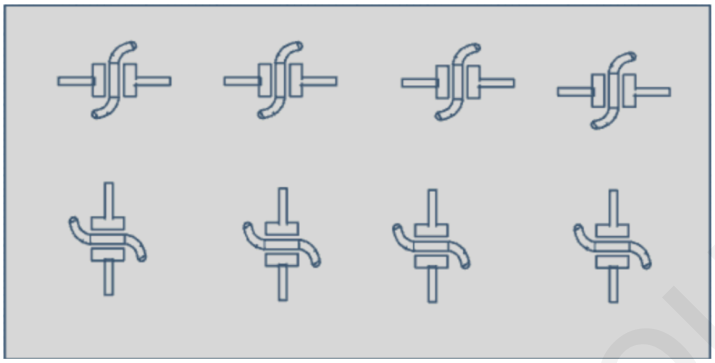

Figure 3.4: A representation of the slab with the designs.

A representation of the single layer design with measurements is shown in Fig. 3.5. The design was finalized based on what it was commonly described in the literature review but also what our team discovered to work best during our trials with different characteristics. Some of those where, the ratio between the silicon base and the curing agent of the PDMS, the distance between the central channel and the vacuum chambers but also the shape of the central channel.

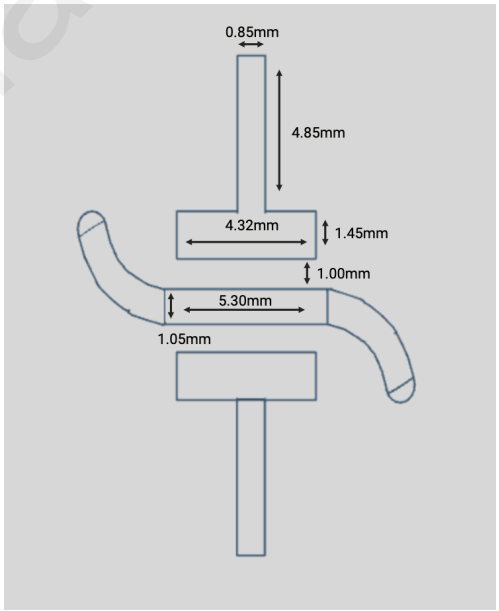

Figure 3.5: Detailed representation of the design's dimensions.

3.3 3D printing

In order to proceed with the printing of the designed slab, we first exported from Tinkercad the design to an OBJ (.obj) file. This is the expected input format on the Chitubox software that was used next. Chitubox is a software tool that helped us pre-process and evaluated the 3D mold before actually printing it. This tool provides useful information about the design and the printing process (e.g. the printing time, the option to 'slice' the design and see the layers in each slice and many more). Then, we exported the design in '.photon' file from Chitubox and transfered it on the 3D printer Fig. 3.6.

Before printing, there are some steps to follow that assure the successful completion of the printing process. First, we checked that the head of the printer was fully cleaned without any resin remaining and that it was properly aligned in a straight position parallel to the base. After, we poor the resin inside the base making sure to not filling it up to the top that might lead to overflow during the process. Then, we could select the imported design and start printing. The process can take up to some hours, at each moment we were able to see the printing status on the printer's screen.

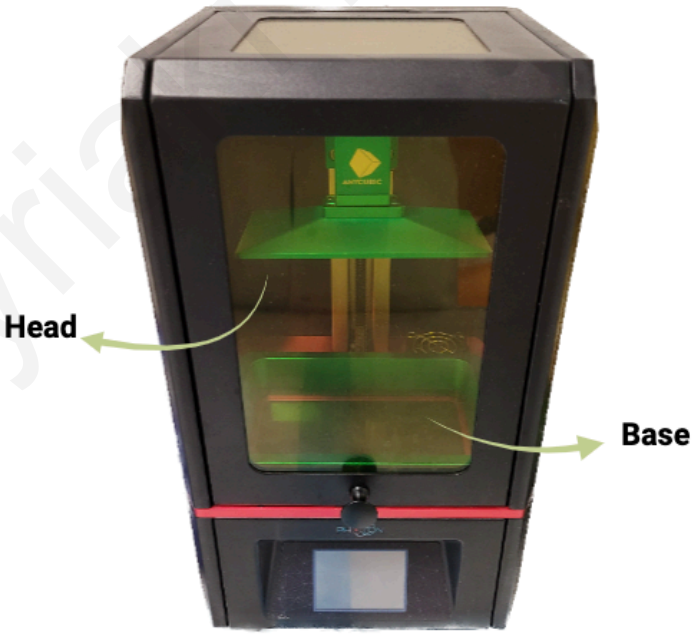

Figure 3.6: The ANYCUBIC 3D printer that we used for printing the mold.

After the printing was completed, the mold was carefully removed from the head with a spatula. Then, we used the Washing and Curing machine to clean and cure

any resin remaining from the mold. First we placed the mold into the basket of the machine shown in Fig.3.7.a for washing. The process was repeated until we considered that the mold was fully cleaned. Then we removed the basket and placed the mold with the side containing the designs, upward and we set off the curing process for six minutes (Fig.3.7.b). The purpose of this process is to cure or differently "dry" any resin remaining from the product using UV (ultraviolet light).

The mold as shown in the Fig.3.8, could be used for the next step of the process.

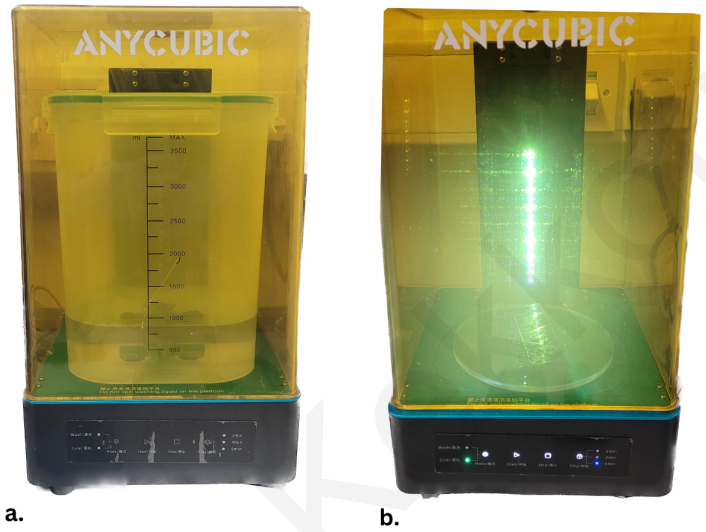

Figure 3.7: ANYCUBIC Wash and Cure machine, based on the selected option it can wash or cure the the 3D object that was printed. There are different duration times 2,4 and 6 minutes for both processes. (a) The image shows the machine with the essential tools for washing the mold. The plastic container has isopropanol that is spinned during the washing by the propeller in the bottom. This helps to remove the remaining resin off the mold. (b) The machine during the curing process. The curing process is important in order for the object to solidify. Since the resin is UV reactive the hood of the machine designed to block it and helps the solidification process.

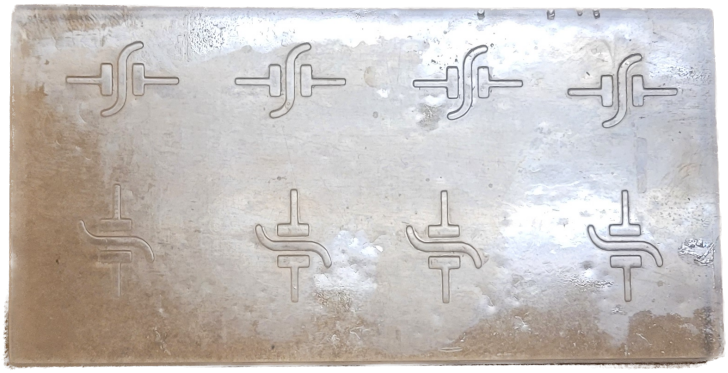

Figure 3.8: The mold that was designed and produced for the purposes of this project. It has eight structures that create four devices.

3.4 Soft Lithography

The mold that was designed and printed, it was used to fabricate the PDMS by soft lithography. Soft lithography technique is a process of fabricating - replicating a structure by embossing an elastomer on a mold. The detailed process of preparing the PDMS and developing the device's PDMS layers is explained in the appendix A. After we had prepared the layers of each device we could proceed with the device assemble.

3.5 Device assembly

After finishing with the process of soft lithography we can eventually assemble the device. The device is assembled in the same way as the Fig. 3.9 shows.

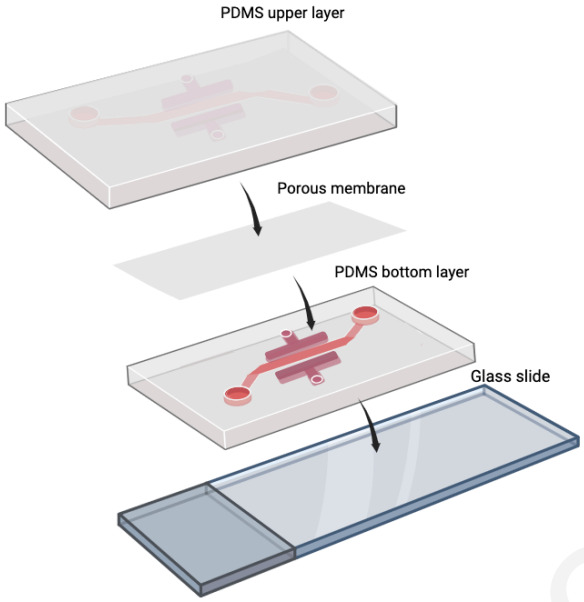

Figure 3.9: Representation of how each component of the device is placed.

The two PDMS layers were attached together and the porous membrane was placed between them. The whole device was placed on the glass slide for better manipulation. The detailed process is described at the appendix B. The completed device is shown in the Fig. 3.10.

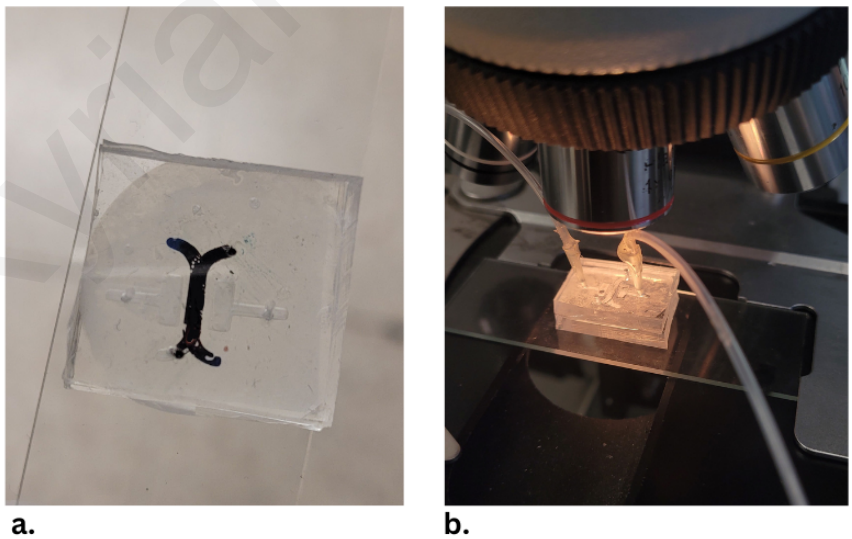

Figure 3.10: Fully developed devices. a)In the image a completed device is shown with the central channel stained by blue and red dye. b)The device under the microscope connected with the actuation mechanism though pipette tips and tubes.

3.6 Actuation

Another important aspect of the gut-on-a-chip device, is the peristaltic-like motion that simulates the movement of the gut. In order to achieve this mechanical actuation, we had set up a system consisting of an Arduino microcontroller board, a relay, an electronic valve and a vacuum pump (Fig. 3.11).

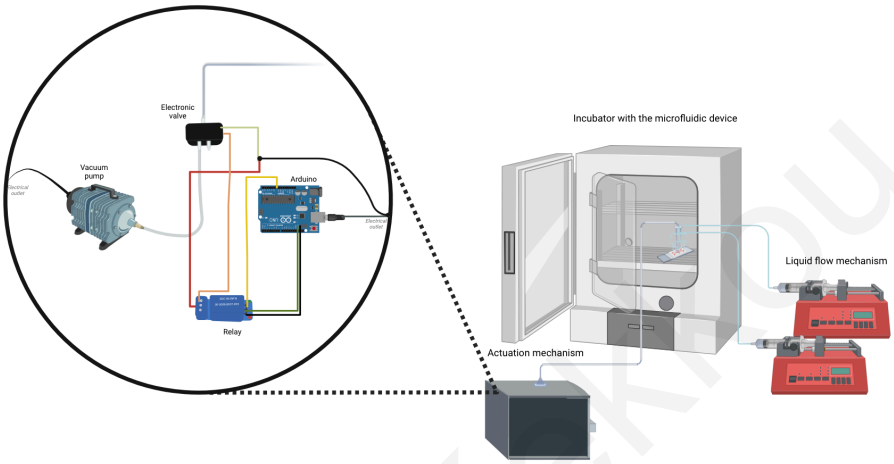

Figure 3.11: The actuation system that enables the peristaltic-like motion. The vacuum pump is responsible for producing the vacuum and the arduino together with the relay and the electronic valve are responsible for the vacuum control.

3.6.1 Microcontroller board

In order for the system to emulate the peristaltic movement of the gut, a controlled vacuum was applied through the vacuum chambers. As mentioned above, during the vacuum application the walls of the central channel are pulled leading to the expansion of the channel. When the vacuum is terminated the channel returns to its initial relaxed state. The expansion and contraction of the central channel looks like the movement of the gut's walls. The vacuum "pulses" are controlled by the Arduino board that communicates with the rest of the components to attain these alternations. Arduino is a microcontroller board that has an embedded Atmel ATmega microcontroller. This board makes the use of the microcontroller a lot easier, since it provides a lot of adds-on like the input and output pins and the Arduino IDE for programming the microcontroller. In the case of this system, we developed a script that sends a signal to the electronic valve through a relay. This signal is basically a switch on signal that

causes the valve to start operating. When a valve is operating, it allows the application of a vacuum on the microfluidic device that lasts six seconds; until Arduino sends another signal, that switches of the valve for a minute. This process is repeated in a loop, while the system is operating. The code can be found in the appendix C.

3.6.2 Pneumatic control

Regarding the production of the vacuum, we used a small vacuum pump (BTC-II Series mini pump), that generates vacuum continuously with vacuum range 0 - 20 in Hg (580mmHg). Since, we didn't want the vacuum to be continuously applied on the device, we attached the outlet of the vacuum pump to the inlet on the electronic valve called Clippard 3-way valve. By using a valve, we could switch on/off the valve and in that way the application of the vacuum.

The valve's outlet tube was connected through smaller tubes on the vacuum chambers of the microfluidic device. Additionally, electronic connection between the Arduino and the valve was mediated by a relay. A relay is able to control devices that operate on high voltages, in contrary with Arduino that can directly control devices with working voltage 5V. Thus, the relay receives the signals from Arduino and then transfers them to the electronic valve. The pneumatic control is summarized at the Fig. 3.12.

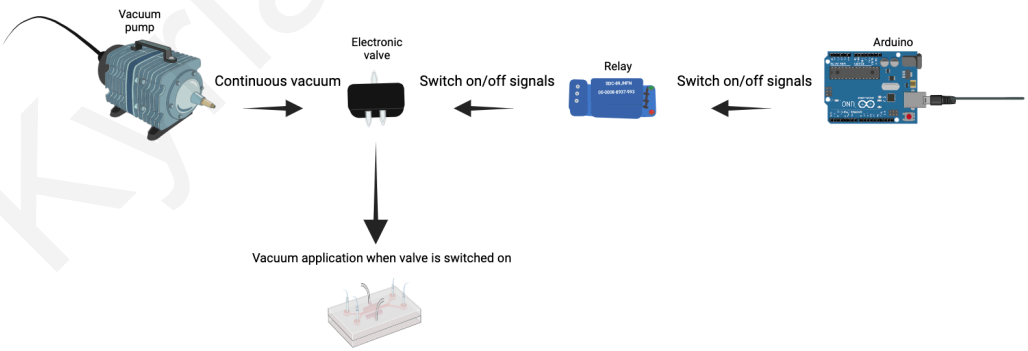

Figure 3.12: Simplified representation of the communication between the different parts that enable the pneumatic control.

3.7 System assembly

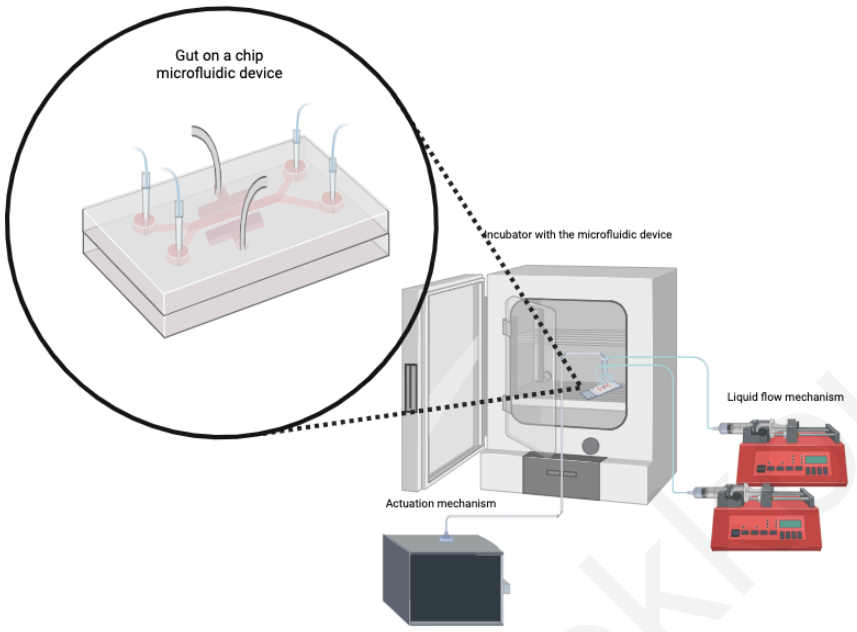

Figure 3.13: The completed set-up for the gut-on-a-chip system ready for use.

Finally, the last step of the process was to put everything together, preparing the device for use. First, we placed the tubes on the device for both the fluid flow and the actuation mechanism. The tube's diameters between the different components differ so we adjusted everything using adapters and glue for stabilization and prevention of leakages. For the vacuum, we joined the outlet of the electrical valve with the vacuum chambers of the device. Also for the fluid flow, joined the tubes from the Alladin pumps to the inlets and outlets of the device.

After everything we described was in place, the system was ready for use. The illustration in Fig. 3.13 shows completed set-up, with the device ready to be seeded with cells. In the Fig. 3.14 the actual, actuation mechanism we have set up and the connections between the components are shown. The device can also be seen connected with the actuation mechanism through the tubes and pipettes tips on the vacuum chambers.

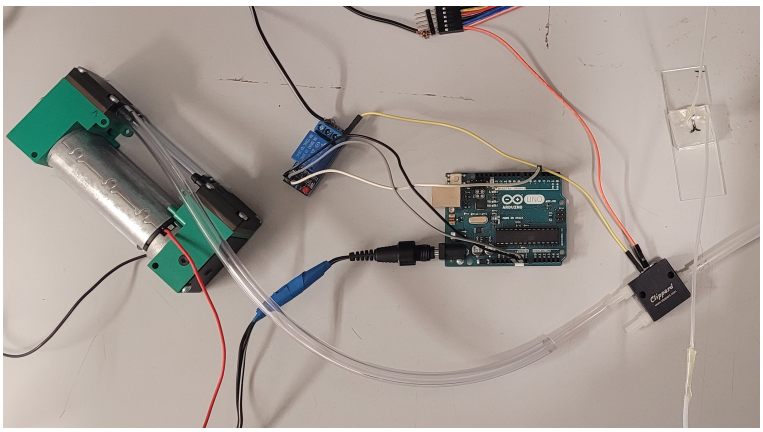

Figure 3.14: The pneumatic actuation of the system connected with the microfluidic device. The pneumatic actuation as described consist of the vacuum pump producting the continuous vacuum, the electronic valve that controls the flow of air and interchangably the application of the vacuum on the device, the relay that mediated the comminication between the valve and the arduino board and finally the arduino that manages the the frequency and duration of vacuum application.

For the purposes of testing and evaluate the percentage of the peristaltic-like movement of the device, we have used a microscope and a software tool to capture videos during the activation of the pneumatic mechanism. As shown in the Fig. 3.15, we took videos of the central channel that were used during the image analysis.

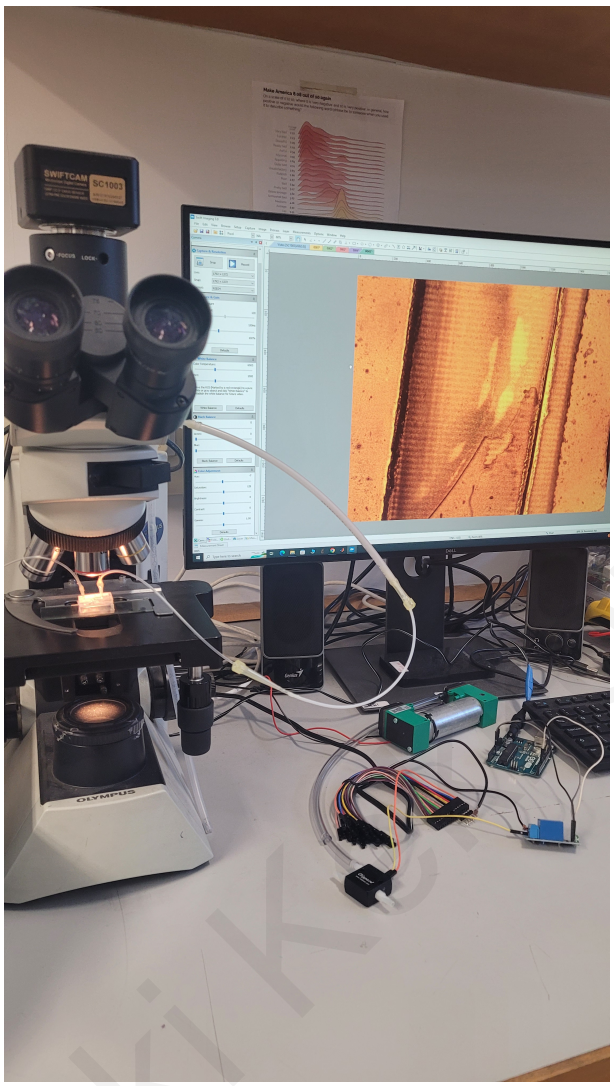

Figure 3.15: The video acquisition was carried out by the use of an optical microsopy connected to a camera, which was also connected with a software installed on the computer, that enables the image/video capture and manipulation. In order to calculate the expansion of the channel during the pneumatic actuation, we used image processing techiques. For this purpose, we took multiple videos during the pneumatic actuation, these videos were used as an input to the image processing script. The set up for the video acquisition is shown in the image, on the display we can see the device's central channel.

Chapter 4

Validation via Image Analysis

Image Analysis is an important aspect of that project that provided helpful insights about the movement of device's central channel during vacuum application. The idea was to develop a script that could calculate the central's channel expansion by measuring its initial width and the expanded one caused by the vacuum application and then find the percentage of the expansion. For the purposes of image analysis we have written a script in Matlab, that offers a lot of useful tools for image processing and analysis.

4.1 Background

4.1.1 Gaussian smoothing filter

Gaussian is a smoothing low pass filter that reduces noise and details by reducing the high frequencies of an image. The Gaussian smoothing operator is a 2D convolution operator (Fig. 4.1) that uses a kernel that is used to calculate the new value of each pixel of an image. The kernel is calculated based on the Gaussian distribution given by the formula 4.1 . Gaussian filter is consider isotropic since it has the same standard deviation in both dimensions. The standard deviation determines the width of the distribution.

$$G(x) = \frac{1}{\sqrt{2\pi}\sigma} e^{-\frac{x^2}{2\sigma^2}} \tag{4.1}$$

$$G(x, y) = \frac{1}{2\pi\sigma^2} e^{-\frac{x^2+y^2}{2\sigma^2}} \tag{4.2}$$

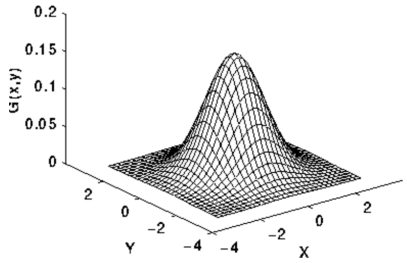

Figure 4.1: Gaussian isotropic distribution, with mean (0,0) and σ=1. Image from [131]

The values of that distribution are used to create the convolution matrix/kernel Fig. 4.2. Then the convolution matrix is applied in the image, for each pixel a new value is calculate by the weighted average of the adjacent pixels. This distribution gives more weight on the central pixels and less to the neighboring ones based on their distance from the original pixel. An example of the gaussian smoothing filter is shown in Fig. 4.3

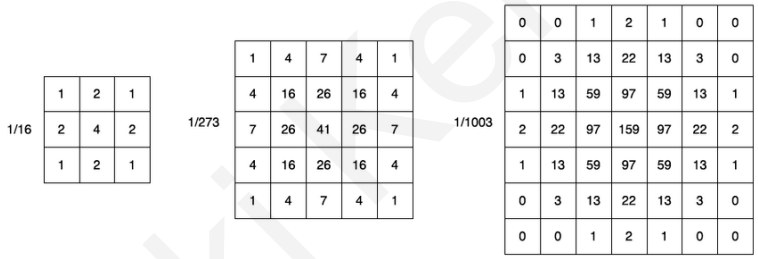

Figure 4.2: Example of the Gaussian kernels .

Figure 4.3: The cameraman is an image used excessively for image processing. Here is the original image and an example of Gaussian smoothed image with sigma value of 3.

The higher standard deviation value we have, a higher degree of smoothing will take place. The value of sigma should be evaluated based on the application and the

image we need to smooth.

4.1.2 Sobel Edge Detection

Edge detection is a technique used in image processing to find edges and discontinuities in images. Is a handful tactic, when we want to focus in a specific feature of the image instead of the rest of the details. Edges are consider the points of the image that sharp brightness differences exist. The most common Edge detection algorithms are Sobel, Canny, Prewitt, Roberts.

The Sobel edge detection filter uses two different 3x3 kernels Fig. 4.4 to estimate the gradients in x-direction and y-direction. The image is processed in each direction separately, by convoluting the image with each mask. Then a new image is created from the summation of the Gx and Gy images.

X – Direction Kernel

-1	0	1
-2	0	2
-1	0	1

Y – Direction Kernel

-1	-2	-1
0	0	0
1	2	1

Figure 4.4: The two kernels in the X and Y direction.

Since in the kernels there are both negative and positive numbers the results of the Gx and Gy images they will contain negative and positives numbers as well, thus the combination of gradients is given by the equation in 4.3. An example of the result of sobel algorithm is shown in Fig. 4.5.

$$G = \sqrt{G_x^2 + G_y^2} \tag{4.3}$$

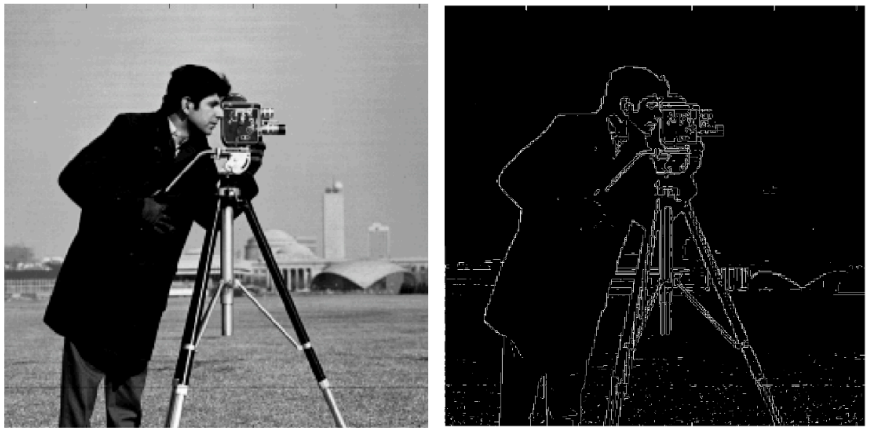

Figure 4.5: Sobel edge detection example.

4.2 Methodology

The script takes as an input, a video which must present the device's main channel during the peristaltic motion. Then the video is broken into frames where each frame is processed separately.

Firstly, each frame is transformed into a gray-scale image so it can be used by the Gaussian smoothing filter. The Gaussian smoothing filter as described above is used to smooth out details and noise. Since the videos where taken under the microscope and there was motion in the device, there are many artifacts and noise in each image that interfere with the edge detection and consequently with the identification of the channel. By applying the Gaussian smoothing filter we eliminate useless information from the image and we can see that the edges are constituted mainly by the channel's walls. Also, by changing the sigma parameter of Gaussian filter we have identified significant differences in the final results of edge detection. The smoothed image is then converted to black and white image and it is used as an input to the Sobel edge detection filter.

The function that implements the Sobel filter other than the resulted image, returns two matrices, the horizontal (Gy) and vertical (Gx) gradients as well. The vertical gradient offers useful information about the positioning of edges and we consider that the columns with higher gradient contain the channel's wall. Then we found the column with higher gradient on the first part of the image considering it as the first wall and then doing the same on the second part of the image to find the second wall.By these

means, we can calculate the distance between the two columns by selecting two parallel points on each column.

After finding the width of the channel in each frame of the video we compare the initial with of the channel with the largest width that was calculated. This result constitutes the percentage of the channel's expansion during the vacuum application.

4.3 Results

4.3.1 Manual Measurements

In order to validate the peristaltic-like motion of the channel, we have carried out many experiments with different devices of different characteristics but also different vacuum values. The movement in the central channel was successfully emulated and captured in the videos through microscope. The maximum expansion of the central channel was 2.1% and it was measured during our experiments with vacuum value of 23inHg (Inch of mercury). In the Fig. 4.6 a representative application is shown, with the channel in the relaxed and expanded state.

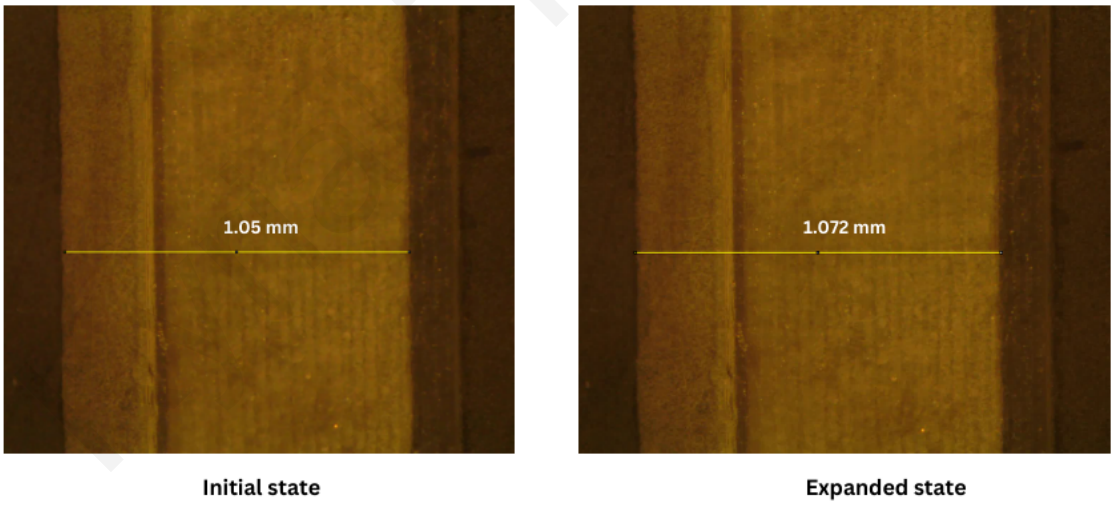

Figure 4.6: Manual measurement of the central's channel width both in relax and expanded state. This resulting to an expansion of a percentage 2.1%.

Based on what we have mentioned in the literature review, the expected mechanical deformation of the Caco-2 cells is 10%. Based on each specific application and the needs of different cells the deformation percentage might differs. On this case, the mechanical deformation of the Caco-2 cells can be investigated further in another project, since

we have accomplished the deformation in the channel's level. It is important to note that, that the resulted strain - the amount of deformation as a response to a specific stress might differs between different materials. That been said, the amount of strain in the Caco-2 cells it might be different from that of the central channel with the same amount of vacuum.

4.3.2 Measurements using image analysis

The next step to the process was to test our script using the same data and evaluate its effectiveness. Each frame from the video undergoes the same processing in order to calculate the result, this process is shown step by step in the Fig. 4.7

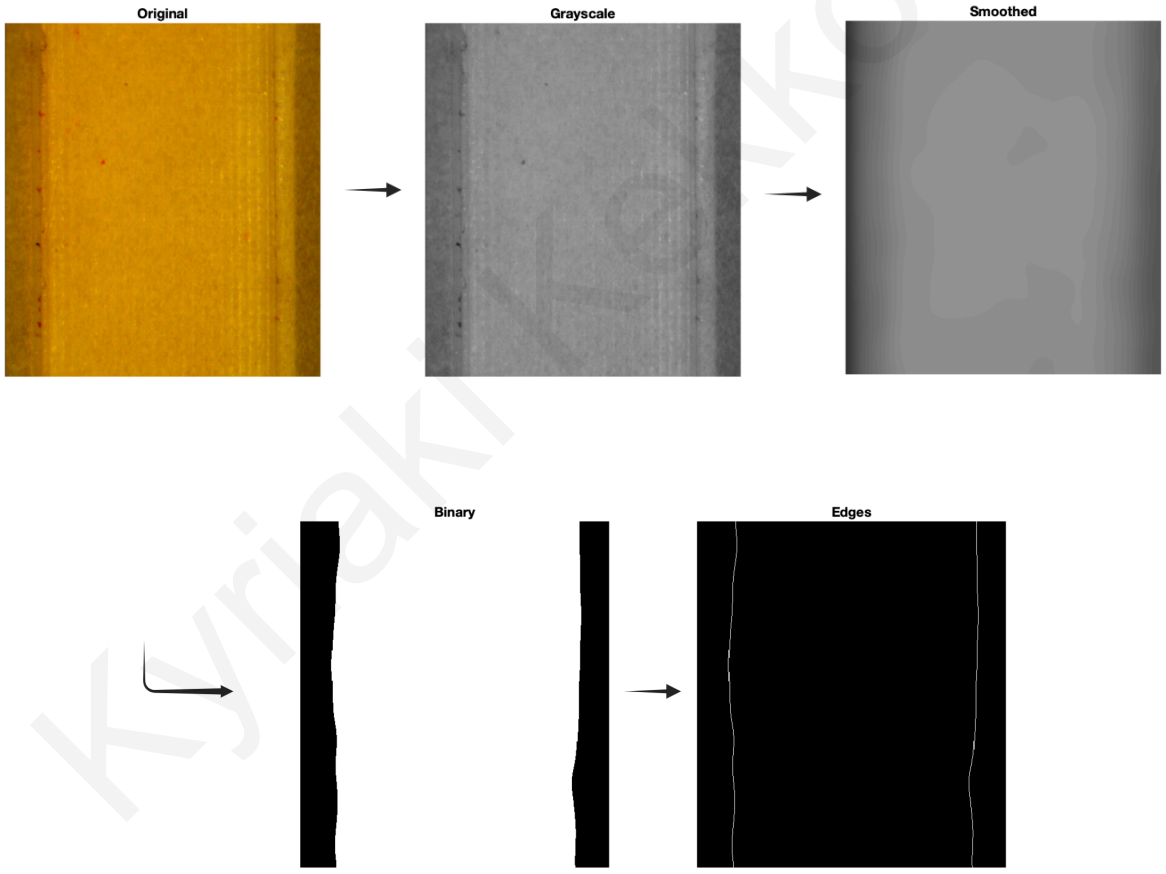

Figure 4.7: The processing that every frame is going through in order to calculate the distance. The initial image is converted to grayscale and then is smoothed with the Gaussian smoothing filter. The smoothed image is transform to binary by using Otsu's threshold method. The final step is to find the edges of the image that will indicate the channel's walls.

Standard deviation experimentation

The sigma (σ) which is the Standard Deviation of the Gaussian Smoothing filter is the variable parameter that affects how effectively the Sobel filter will work and identify the correct edges. In our tests we have experimented with different sigma values to evaluate which works best in our case. The results of the different experiments are shown in the Fig. 4.8. The channel's edges were identified more accurately with $\sigma = 15$.

Figure 4.8: In this experiments we can clearly see that while the sigma value is increasing the detection of edges is more accurate and the wall's of the central channel are defined clearly. Around 15 and above we see that by increasing the sigma we don't have particular changes in the final result.

In order to decide the preferred value for σ, we needed the completed results produced by the script. Thus, we run our script that calculates the percentage of change of the channel when a vacuum is applied and compare it to the width of the channel we calculated manually.

In more detail the script exports useful data regarding the channel's width during the video. These data are, the number of the frame that was found having the smallest width and this width likewise the number of the frame with the largest width calculated and this width. In addition to that the calculated difference and the percentage of expansion are also exported. In the Table. 4.1 there are some of the information mentioned above.

On that table the same video that we calculated manually was used as an input to

Sigma	Smallest channel's width	Largest channel's width	Expansion %
35	1008	1016	0.79
20	1007	1018	1.09
15	1007	1016	0.89
10	1011	1018	0.69
5	733	737	0.55
1	733	739	0.82

Table 4.1: Example results of a testing we carried out with a video of the channel. In the video the channel was relaxed and then we applied vacuum.

the script. On these data there aren't specific patterns following the change of sigma. But, we can see that when the σ=15, the results are closer to what we have calculated manually. As we can seen in the resulted images in Fig. 4.8, when σ <=10, many image artifacts are considered edges and might affect the final results during the identification of the two walls. In order set an upper bound to the value of sigma we also wanted to check when the smoothing is way to much that again might lead to wrong results. In that case we wanted to check the specific frames that the smallest/largest channel's width were found and inspect which was the image's columns with the higher gradient, since the columns with the higher gradient in our code are consider the walls of the channel. We consider that when the σ >35 the smoothing leads to lost of details that again lead to wrong identification of the walls channels, leading to wrong results.

Chapter 5

Conclusion

The prospects of organ-on-chip platforms to replace the currently used methods for experimentation and tests of drugs and therapeutics are widely recognized in the research community. Likewise, the system we have successfully developed can be used as a tool for any gut-related research, since is flexible enough to support different types of cells, bacteria and medium substances to either investigate healthy or pathogenic conditions. Clearly, some of the characteristics can be altered to support different concepts, but the tool can help the further investigation of the gut and more importantly enable us to further progress the research for new drugs and therapeutics of gut cancer and other diseases.

This multidisciplinary project, has offered us a lot of knowledge in multiple tools that will be undoubtedly very useful in the future and the next steps in our career. Beginning with the ability to design and print items using 3D design tools and the 3D printer. Likewise, it gave us the chance to learn the soft lithography technique to replicate structures in elastomer using a mold; a method that can be used is many different fields and it provided the foundation to learn other similar techniques. The process of bringing together different components to enable the mechanical actuation, brought new insights about unknown, till then components and how they work; in combination with the knowledge of vacuum production and the vacuum characteristics. The need to evaluate the motion of the channel, has led us to learn how to use the microscope and acquire videos and photos of the device. In addition to that, for the purposes of image analysis, we have research the edge detection algorithms and decided to use Matlab that facilitates the coding, with the Image Processing Toolbox. Last but not least, this project presupposes an understanding in gut physiology in order to

emulate its environment and have a deeper understanding on what we really wanted to develop.

Undoubtedly, there are things on the project we could do different in order to have better overall results. One of this is the use of a different vacuum pump with ability to produce higher values of vacuum (which is actually below -20inHg). This might result to higher expansion of the central channel. In combination with that, we could test devices developed with different percentage of silicon elastomer base to curing agent. Instead of 10:1, we could test higher ratio of elastomer (ex. 12:1), that would result to more elastic devices, thus, less vacuum. In addition to that, we could make some alterations to the code for image analysis for more precise results. Specifically, we could change the way the channel's walls are identified by taking into consideration the changes of gradient in the whole frame in order to conclude which is the column containing the wall.

Since the concept of organs-on-chip is still in the very beginning at the research level, there are many pathways someone can follow to investigate further their use or experiment with drugs and treatments. Specifically, this system can be used to be seeded with cells and bacteria in order to complete the gut-on-a-chip concept as described in the work of Kim et al. [38]. It is crucial to test that cells can grow and remain viable in the device and also to evaluate the composition of the provided medium and its flow rate. In addition to these, the actuation set up should be tested and it's variables to be adjusted to provide the 10% expansion to the cells in order for them to obtain the expected shape and gradually to recreate a villi like structure. Finally, when the gut-on-a-chip system is completed it can be used for any gut-related experimentation and drug tests. With the hope, that these devices will eventually replace the animal tests and they can be a reliable and personalized tool for gut illnesses and especially gut cancer.

Bibliography

[1] D. Van Wynsberghe, R. Carola, and C.R. Noback. Human Anatomy and Physiology. McGraw-Hill, 1995.

[2] Your Digestive System & How it Works, 2017.

[3] Ifeanyichukwu Ogobuiro, Justin Gonzales, Karlie R Shumway, and Faiz Tuma. Physiology, gastrointestinal. In StatPearls. StatPearls Publishing, Treasure Island (FL), January 2024.

[4] What are the layers of the gastrointestinal tract what are their functions.

[5] Abijain. Understanding the gastrointestinal system: A guide to the organs, functions, and common conditions, Apr 2023.

[6] Dimple Palanilkunnathil Thomas, Jun Zhang, Nam-Trung Nguyen, and Hang Thu Ta. Microfluidic gut-on-a-chip: Fundamentals and challenges. Biosensors, 13(1), 2023.

[7] Digestive system of humans explained with diagrams, Dec 2023.

[8] Physiology of the digestive system, May 2016.

[9] Inna Sekirov, Shannon L Russell, L Caetano M Antunes, and B Brett Finlay. Gut microbiota in health and disease. Physiological reviews, 2010.

[10] Grissel Trujillo-de Santiago, Matías José Lobo-Zegers, Silvia Lorena Montes-Fonseca, Yu Shrike Zhang, and Mario Moisés Alvarez. Gut-microbiota-on-a-chip: an enabling field for physiological research. Microphysiological systems, 2, 2018.

[11] Elizabeth Thursby and Nathalie Juge. Introduction to the human gut microbiota. Biochemical journal, 474(11):1823–1836, 2017.

[12] Gut Microbiome, Aug 2023.

[13] Melina Arnold, Christian C Abnet, Rachel E Neale, Jerome Vignat, Edward L Giovannucci, Katherine A McGlynn, and Freddie Bray. Global burden of 5 major types of gastrointestinal cancer. Gastroenterology, 159(1):335–349, 2020.

[14] Silvia Rodrigues Jardim, Lucila Marieta Perrotta de Souza, and Heitor Siffert Pereira de Souza. The rise of gastrointestinal cancers as a global phenomenon: Unhealthy behavior or progress? International Journal of Environmental Research and Public Health, 20(4), 2023.

[15] Miranda M Fidler, Freddie Bray, Salvatore Vaccarella, and Isabelle Soerjomataram. Assessing global transitions in human development and colorectal cancer incidence. International journal of cancer, 140(12):2709–2715, 2017.

[16] Maomao Cao, He Li, Dianqin Sun, Siyi He, Xinxin Yan, Fan Yang, Shaoli Zhang, Changfa Xia, Lin Lei, Ji Peng, et al. Current cancer burden in china: epidemiology, etiology, and prevention. Cancer biology & medicine, 19(8):1121, 2022.

[17] Filippo Vernia, Salvatore Longo, Gianpiero Stefanelli, Angelo Viscido, and Giovanni Latella. Dietary factors modulating colorectal carcinogenesis. Nutrients, 13(1):143, 2021.

[18] Piet A van den Brandt. The impact of a healthy lifestyle on the risk of esophageal and gastric cancer subtypes. European Journal of Epidemiology, 37(9):931–945, 2022.

[19] Alex Chung, Lucy Westerman, Jane Martin, and Sharon Friel. The commercial determinants of unhealthy diets. Public Health Research & Practice, 32(3), 2022.

[20] Véronique Bouvard, Dana Loomis, Kathryn Z Guyton, Yann Grosse, Fatiha El Ghissassi, Lamia Benbrahim-Tallaa, Neela Guha, Heidi Mattock, and Kurt Straif. Carcinogenicity of consumption of red and processed meat. The Lancet Oncology, 16(16):1599–1600, 2015.

[21] Andrew G Renehan, Margaret Tyson, Matthias Egger, Richard F Heller, and Marcel Zwahlen. Body-mass index and incidence of cancer: a systematic review and meta-analysis of prospective observational studies. The lancet, 371(9612):569–578, 2008.

[22] Farhad Islami, Ann Goding Sauer, Kimberly D Miller, Rebecca L Siegel, Stacey A Fedewa, Eric J Jacobs, Marjorie L McCullough, Alpa V Patel, Jiemin Ma, Isabelle Soerjomataram, et al. Proportion and number of cancer cases and deaths attributable to potentially modifiable risk factors in the united states. CA: a cancer journal for clinicians, 68(1):31–54, 2018.

[23] Christina Fitzmaurice, Christine Allen, Ryan M Barber, Lars Barregard, Zulfiqar A Bhutta, Hermann Brenner, Daniel J Dicker, Odgerel Chimed-Orchir, Rakhi Dandona, Lalit Dandona, et al. Global, regional, and national cancer incidence, mortality, years of life lost, years lived with disability, and disability-adjusted life-years for 32 cancer groups, 1990 to 2015: a systematic analysis for the global burden of disease study. JAMA oncology, 3(4):524–548, 2017.

[24] Hyuna Sung, Rebecca L Siegel, Philip S Rosenberg, and Ahmedin Jemal. Emerging cancer trends among young adults in the usa: analysis of a population-based cancer registry. The Lancet Public Health, 4(3):e137–e147, 2019.

[25] Emily Harrold, Alicia Latham, Naveen Pemmaraju, and Christopher H. Lieu. Early-onset gi cancers: Rising trends, genetic risks, novel strategies, and special considerations. American Society of Clinical Oncology Educational Book, (43):e398068, 2023. PMID: 37235819.

[26] Rebecca L Siegel, Kimberly D Miller, Hannah E Fuchs, and Ahmedin Jemal. Cancer statistics, 2022. CA: a cancer journal for clinicians, 72(1):7–33, 2022.

[27] Tomasz Sawicki, Monika Ruszkowska, Anna Danielewicz, Ewa Niedzwiedzka, Tomasz Arłukowicz, and Katarzyna Przybyłowicz. A review of colorectal cancer in terms of epidemiology, risk factors, development, symptoms and diagnosis. Cancers, 13:2025, 04 2021.

[28] Marzieh Araghi, Isabelle Soerjomataram, Aude Bardot, Jacques Ferlay, Citadel J Cabasag, David S Morrison, Prithwish De, Hanna Tervonen, Paul M Walsh, Oliver Bucher, et al. Changes in colorectal cancer incidence in seven high-income countries: a population-based study. The lancet Gastroenterology & hepatology, 4(7):511–518, 2019.

[29] Fanny ER Vuik, Stella AV Nieuwenburg, Marc Bardou, Iris Lansdorp-Vogelaar, Mário Dinis-Ribeiro, Maria J Bento, Vesna Zadnik, María Pellisé, Laura Esteban, Michal F Kaminski, et al. Increasing incidence of colorectal cancer in young adults in europe over the last 25 years. Gut, 68(10):1820–1826, 2019.

[30] Rebecca L Siegel, Stacey A Fedewa, William F Anderson, Kimberly D Miller, Jiemin Ma, Philip S Rosenberg, and Ahmedin Jemal. Colorectal cancer incidence patterns in the united states, 1974–2013. JNCI: Journal of the National Cancer Institute, 109(8):djw322, 2017.

[31] Catherine de Martel, Damien Georges, Freddie Bray, Jacques Ferlay, and Gary M Clifford. Global burden of cancer attributable to infections in 2018: a worldwide incidence analysis. The Lancet Global Health, 8(2):e180–e190, 2020.

[32] Edoardo Botteri, Simona Iodice, Vincenzo Bagnardi, Sara Raimondi, Albert B Lowenfels, and Patrick Maisonneuve. Smoking and colorectal cancer: a meta-analysis. Jama, 300(23):2765–2778, 2008.

[33] Martin CS Wong, CH Chan, Jiayan Lin, Jason LW Huang, Junjie Huang, Yuan Fang, Wilson WL Cheung, CP Yu, John CT Wong, Gary Tse, et al. Lower relative contribution of positive family history to colorectal cancer risk with increasing age: a systematic review and meta-analysis of 9.28 million individuals. The American Journal of Gastroenterology, 113(12):1819, 2018.

[34] Claudia Allemani, Tomohiro Matsuda, Veronica Di Carlo, Rhea Harewood, Melissa Matz, Maja Nikšić, Audrey Bonaventure, Mikhail Valkov, Christopher J Johnson, Jacques Estève, et al. Global surveillance of trends in cancer survival 2000–14 (concord-3): analysis of individual records for 37 513 025 patients diagnosed with one of 18 cancers from 322 population-based registries in 71 countries. The Lancet, 391(10125):1023–1075, 2018.

[35] Béatrice Lauby-Secretan, Nadia Vilahur, Franca Bianchini, Neela Guha, and Kurt Straif. The iarc perspective on colorectal cancer screening. New England Journal of Medicine, 378(18):1734–1740, 2018.

[36] Eline H Schreuders, Arlinda Ruco, Linda Rabeneck, Robert E Schoen, Joseph JY Sung, Graeme P Young, and Ernst J Kuipers. Colorectal cancer screening: a global overview of existing programmes. Gut, 64(10):1637–1649, 2015.

[37] Sophie Pilleron, Diana Sarfati, Maryska Janssen-Heijnen, Jérôme Vignat, Jacques Ferlay, Freddie Bray, and Isabelle Soerjomataram. Global cancer incidence in older adults, 2012 and 2035: a population-based study. International journal of cancer, 144(1):49–58, 2019.

[38] Hyun Jung Kim, Dongeun Huh, Geraldine Hamilton, and Donald E Ingber. Human gut-on-a-chip inhabited by microbial flora that experiences intestinal peristalsis-like motions and flow. Lab on a Chip, 12(12):2165–2174, 2012.

[39] Amin Valiei, Javad Aminian-Dehkordi, and Mohammad R. K. Mofrad. Gut-on-a-chip models for dissecting the gut microbiology and physiology. APL Bioengineering, 7(1):011502, 02 2023.

[40] Sasan Jalili-Firoozinezhad, Francesca S Gazzaniga, Elizabeth L Calamari, Diogo M Camacho, Cicely W Fadel, Amir Bein, Ben Swenor, Bret Nestor, Michael J Cronce, Alessio Tovaglieri, et al. A complex human gut microbiome cultured in an anaerobic intestine-on-a-chip. Nature biomedical engineering, 3(7):520–531, 2019.

[41] Woojung Shin, Christopher D Hinojosa, Donald E Ingber, and Hyun Jung Kim. Human intestinal morphogenesis controlled by transepithelial morphogen gradient and flow-dependent physical cues in a microengineered gut-on-a-chip. IScience, 15:391–406, 2019.

[42] Yaqiong Guo, Zhongyu Li, Wentao Su, Li Wang, Yujuan Zhu, and Jianhua Qin. A biomimetic human gut-on-a-chip for modeling drug metabolism in intestine. Artificial Organs, 42(12):1196–1205, 2018.

[43] Jonas Cremer, Igor Segota, Chih-yu Yang, Markus Arnoldini, John T Sauls, Zhongge Zhang, Edgar Gutierrez, Alex Groisman, and Terence Hwa. Effect of flow and peristaltic mixing on bacterial growth in a gut-like channel. Proceedings of the National Academy of Sciences, 113(41):11414–11419, 2016.

[44] Massimo Marzorati, Barbara Vanhoecke, Tine De Ryck, Mehdi Sadaghian Sadabad, Iris Pinheiro, Sam Possemiers, Pieter Van den Abbeele, Lara Derycke, Marc Bracke, Jan Pieters, et al. The hmi™ module: a new tool to study the host-microbiota interaction in the human gastrointestinal tract in vitro. BMC microbiology, 14:1–14, 2014.

[45] Pranjul Shah, Joëlle V Fritz, Enrico Glaab, Mahesh S Desai, Kacy Greenhalgh, Audrey Frachet, Magdalena Niegowska, Matthew Estes, Christian Jäger, Carole Seguin-Devaux, et al. A microfluidics-based in vitro model of the gastrointestinal human–microbe interface. Nature communications, 7(1):11535, 2016.

[46] Kyu-Young Shim, Dongwook Lee, Jeonghun Han, Nam-Trung Nguyen, Sungsu Park, and Jong Hwan Sung. Microfluidic gut-on-a-chip with three-dimensional villi structure. Biomedical microdevices, 19(2):37, 2017.

[47] Yong Cheol Shin, Woojung Shin, Domin Koh, Alexander Wu, Yoko M Ambrosini, Soyoun Min, S Gail Eckhardt, RY Declan Fleming, Seung Kim, Sowon Park, et al. Three-dimensional regeneration of patient-derived intestinal organoid epithelium in a physiodynamic mucosal interface-on-a-chip. Micromachines, 11(7):663, 2020.

[48] Magdalena Kasendra, Alessio Tovaglieri, Alexandra Sontheimer-Phelps, Sasan Jalili-Firoozinezhad, Amir Bein, Angeliki Chalkiadaki, William Scholl, Cheng Zhang, Hannah Rickner, Camilla A. Richmond, Hu Li, David T. Breault, and Donald E. Ingber. Development of a primary human small intestine-on-a-chip using biopsy-derived organoids. Scientific Reports, 8(1):2871, Feb 2018.

[49] Jeongyun Kim, Manjunath Hegde, and Arul Jayaraman. Co-culture of epithelial cells and bacteria for investigating host–pathogen interactions. Lab on a Chip, 10(1):43–50, 2010.

[50] A Tovaglieri, A Sontheimer-Phelps, A Geirnaert, R Prantil-Baun, DM Camacho, DB Chou, S Jalili-Firoozinezhad, T de Wouters, M Kasendra, M Super, et al. Species-specific enhancement of enterohemorrhagic e. coli pathogenesis mediated by microbiome metabolites. microbiome 1–59, 2019.

[51] Alexandre Grassart, Valérie Malardé, Samy Gobaa, Anna Sartori-Rupp, Jordan Kerns, Katia Karalis, Benoit Marteyn, Philippe Sansonetti, and Nathalie Sauvonnet. Bioengineered human organ-on-chip reveals intestinal microenvironment and mechanical forces impacting shigella infection. Cell host & microbe, 26(3):435–444, 2019.

[52] Yaqiong Guo, Ronghua Luo, Yaqing Wang, Pengwei Deng, Tianzhang Song, Min Zhang, Peng Wang, Xu Zhang, Kangli Cui, Tingting Tao, et al. Sars-cov-2 induced intestinal responses with a biomimetic human gut-on-chip. Science bulletin, 66(8):783–793, 2021.

[53] Hyun Jung Kim, Hu Li, James J Collins, and Donald E Ingber. Contributions of microbiome and mechanical deformation to intestinal bacterial overgrowth and inflammation in a human gut-on-a-chip. Proceedings of the National Academy of Sciences, 113(1):E7–E15, 2016.

[54] Mary E Wikswo, Nino Khetsuriani, Ashley L Fowlkes, Xiaotian Zheng, Silvia Penaranda, Natasha Verma, Stanford T Shulman, Kanta Sircar, Christine C Robinson, Terry Schmidt, et al. Increased activity of coxsackievirus b1 strains associated with severe disease among young infants in the united states, 2007—2008. Clinical Infectious Diseases, 49(5):e44–e51, 2009.

[55] Remi Villenave, Samantha Q Wales, Tiama Hamkins-Indik, Efstathia Papafragkou, James C Weaver, Thomas C Ferrante, Anthony Bahinski, Christopher A Elkins, Michael Kulka, and Donald E Ingber. Human gut-on-a-chip supports polarized infection of coxsackie b1 virus in vitro. PloS one, 12(2):e0169412, 2017.

[56] Sasan Jalili-Firoozinezhad, Rachelle Prantil-Baun, Amanda Jiang, Ratnakar Potla, Tadanori Mammoto, James C Weaver, Thomas C Ferrante, Hyun Jung Kim, Joaquim MS Cabral, Oren Levy, et al. Modeling radiation injury-induced cell death and countermeasure drug responses in a human gut-on-a-chip. Cell death & disease, 9(2):223, 2018.

[57] Vijay K Singh, Patricia LP Romaine, and Victoria L Newman. Biologics as countermeasures for acute radiation syndrome: where are we now? Expert opinion on biological therapy, 15(4):465–471, 2015.

[58] Athanasia Apostolou, Rohit A Panchakshari, Antara Banerjee, Dimitris V Manatakis, Maria D Paraskevopoulou, Raymond Luc, Galeb Abu-Ali, Alexandra Dimitriou, Carolina Lucchesi, Gauri Kulkarni, et al. A novel microphysiological colon platform to decipher mechanisms driving human intestinal permeability. Cellular and Molecular Gastroenterology and Hepatology, 12(5):1719–1741, 2021.

[59] Claudia Beaurivage, Elena Naumovska, Yee Xiang Chang, Edo D Elstak, Arnaud Nicolas, Heidi Wouters, Guido van Moolenbroek, Henriëtte L Lanz, Sebastiaan J Trietsch, Jos Joore, et al. Development of a gut-on-a-chip model for

high throughput disease modeling and drug discovery. International journal of molecular sciences, 20(22):5661, 2019.

[60] Carly Strelez, Sujatha Chilakala, Kimya Ghaffarian, Roy Lau, Erin Spiller, Nolan Ung, Danielle Hixon, Ah Young Yoon, Ren X Sun, Heinz-Josef Lenz, et al. Human colorectal cancer-on-chip model to study the microenvironmental influence on early metastatic spread. Iscience, 24(5), 2021.

[61] Robert S Mccuskey. The hepatic microvascular system in health and its response to toxicants. The Anatomical Record: Advances in Integrative Anatomy and Evolutionary Biology: Advances in Integrative Anatomy and Evolutionary Biology, 291(6):661–671, 2008.

[62] Lawrence A Vernetti, Nina Senutovitch, Robert Boltz, Richard DeBiasio, Tong Ying Shun, Albert Gough, and D Lansing Taylor. A human liver microphysiology platform for investigating physiology, drug safety, and disease models. Experimental biology and medicine, 241(1):101–114, 2016.

[63] Bartholomew J Kane, Michael J Zinner, Martin L Yarmush, and Mehmet Toner. Liver-specific functional studies in a microfluidic array of primary mammalian hepatocytes. Analytical chemistry, 78(13):4291–4298, 2006.

[64] Philip J Lee, Paul J Hung, and Luke P Lee. An artificial liver sinusoid with a microfluidic endothelial-like barrier for primary hepatocyte culture. Biotechnology and bioengineering, 97(5):1340–1346, 2007.

[65] Bahman Delalat, Chiara Cozzi, Soraya Rasi Ghaemi, Giovanni Polito, Frederik H Kriel, Thomas Danny Michl, Frances J Harding, Craig Priest, Giuseppe Barillaro, and Nicolas H Voelcker. Microengineered bioartificial liver chip for drug toxicity screening. Advanced functional materials, 28(28):1801825, 2018.

[66] Danny Bavli, Sebastian Prill, Elishai Ezra, Gahl Levy, Merav Cohen, Mathieu Vinken, Jan Vanfleteren, Magnus Jaeger, and Yaakov Nahmias. Real-time monitoring of metabolic function in liver-on-chip microdevices tracks the dynamics of mitochondrial dysfunction. Proceedings of the National Academy of Sciences, 113(16):E2231–E2240, 2016.

[67] Ken-ichiro Kamei, Momoko Yoshioka, Shiho Terada, Yumie Tokunaga, and Yong Chen. Three-dimensional cultured liver-on-a-chip with mature hepatocyte-like cells derived from human pluripotent stem cells. Biomedical microdevices, 21:1–9, 2019.

[68] Seung-A Lee, Edward Kang, Jongil Ju, Dong-Sik Kim, Sang-Hoon Lee, et al. Spheroid-based three-dimensional liver-on-a-chip to investigate hepatocyte–hepatic stellate cell interactions and flow effects. Lab on a Chip, 13(18):3529–3537, 2013.

[69] Chen-Ta Ho, Ruei-Zeng Lin, Rong-Jhe Chen, Chung-Kuang Chin, Song-En Gong, Hwan-You Chang, Hwei-Ling Peng, Long Hsu, Tri-Rung Yew, Shau-Feng Chang, et al. Liver-cell patterning lab chip: mimicking the morphology of liver lobule tissue. Lab on a Chip, 13(18):3578–3587, 2013.

[70] Fan An, Yueyang Qu, Xianming Liu, Runtao Zhong, and Yong Luo. Organ-on-a-chip: new platform for biological analysis. AnAlyticAl chemistry insights, 10:ACI–S28905, 2015.

[71] Li-Dong Ma, Yi-Tong Wang, Jing-Rong Wang, Jian-Lin Wu, Xian-Sheng Meng, Ping Hu, Xuan Mu, Qiong-Lin Liang, and Guo-An Luo. Design and fabrication of a liver-on-a-chip platform for convenient, highly efficient, and safe in situ perfusion culture of 3d hepatic spheroids. Lab on a Chip, 18(17):2547–2562, 2018.

[72] Manjunath Hegde, Rohit Jindal, Abhinav Bhushan, Shyam Sundhar Bale, William J McCarty, Inna Golberg, O Berk Usta, and Martin L Yarmush. Dynamic interplay of flow and collagen stabilizes primary hepatocytes culture in a microfluidic platform. Lab on a Chip, 14(12):2033–2039, 2014.

[73] Kyungsuk Yum, Soon Gweon Hong, and Luke P Lee. Physiologically relevant organs on chips. Biotechnology journal, 9(1):16, 2014.

[74] Reza Riahi, Seyed Ali Mousavi Shaegh, Masoumeh Ghaderi, Yu Shrike Zhang, Su Ryon Shin, Julio Aleman, Solange Massa, Duckjin Kim, Mehmet Remzi Dokmeci, and Ali Khademhosseini. Automated microfluidic platform of bead-based electrochemical immunosensor integrated with bioreactor for continual monitoring of cell secreted biomarkers. Scientific reports, 6(1):24598, 2016.

[75] Qing Zhou, Dipali Patel, Timothy Kwa, Amranul Haque, Zimple Matharu, Gulnaz Stybayeva, Yandong Gao, Anna Mae Diehl, and Alexander Revzin. Liver injury-on-a-chip: microfluidic co-cultures with integrated biosensors for monitoring liver cell signaling during injury. Lab on a Chip, 15(23):4467–4478, 2015.

[76] Lor Huai Chong, Huan Li, Isaac Wetzel, Hansang Cho, and Yi-Chin Toh. A liver-immune coculture array for predicting systemic drug-induced skin sensitization. Lab on a Chip, 18(21):3239–3250, 2018.

[77] Young Bok Kang, Temitope R Sodunke, Jason Lamontagne, Joseph Cirillo, Caroline Rajiv, Michael J Bouchard, and Moses Noh. Liver sinusoid on a chip: Long-term layered co-culture of primary rat hepatocytes and endothelial cells in microfluidic platforms. Biotechnology and bioengineering, 112(12):2571–2582, 2015.

[78] Dongeun Huh, Benjamin D Matthews, Akiko Mammoto, Martín Montoya-Zavala, Hong Yuan Hsin, and Donald E Ingber. Reconstituting organ-level lung functions on a chip. Science, 328(5986):1662–1668, 2010.

[79] Andreas O Stucki, Janick D Stucki, Sean RR Hall, Marcel Felder, Yves Mermoud, Ralph A Schmid, Thomas Geiser, and Olivier T Guenat. A lung-on-a-chip array with an integrated bio-inspired respiration mechanism. Lab on a Chip, 15(5):1302–1310, 2015.

[80] Mouhita Humayun, Chung-Wai Chow, and Edmond WK Young. Microfluidic lung airway-on-a-chip with arrayable suspended gels for studying epithelial and smooth muscle cell interactions. Lab on a Chip, 18(9):1298–1309, 2018.

[81] Xingyuan Yang, Kaiyan Li, Xu Zhang, Chang Liu, Bingkun Guo, Weijia Wen, and Xinghua Gao. Nanofiber membrane supported lung-on-a-chip microdevice for anti-cancer drug testing. Lab on a Chip, 18(3):486–495, 2018.

[82] Abhishek Jain, Riccardo Barrile, Andries D van der Meer, Akiko Mammoto, Tadanori Mammoto, Karen De Ceunynck, Omozuanvbo Aisiku, Monicah A Otieno, Calvert S Louden, Geraldine A Hamilton, et al. Primary human lung alveolus-on-a-chip model of intravascular thrombosis for assessment of therapeutics. Clinical pharmacology & therapeutics, 103(2):332–340, 2018.

[83] Longlong Si, Haiqing Bai, Melissa Rodas, Wuji Cao, Crystal Yuri Oh, Amanda Jiang, Atiq Nurani, Danni Y Zhu, Girij // i ja Goyal, Sarah E Gilpin, et al. Human organs-on-chips as tools for repurposing approved drugs as potential influenza and covid19 therapeutics in viral pandemics. BioRxiv, 54, 2020.

[84] Jenny Peng, Niels Rochow, Mohammadhossein Dabaghi, Radenka Bozanovic, Jan Jansen, Dragos Predescu, Bryon DeFrance, Sau-Young Lee, Gerhard Fusch, Ponnambalam Ravi Selvaganapathy, et al. Postnatal dilatation of umbilical cord vessels and its impact on wall integrity: prerequisite for the artificial placenta. The International Journal of Artificial Organs, 41(7):393–399, 2018.

[85] Mohammadhossein Dabaghi, Gerhard Fusch, Neda Saraei, Niels Rochow, John L Brash, Christoph Fusch, and P Ravi Selvaganapathy. An artificial placenta type microfluidic blood oxygenator with double-sided gas transfer microchannels and its integration as a neonatal lung assist device. Biomicrofluidics, 12(4), 2018.

[86] Kambez H Benam, Remi Villenave, Carolina Lucchesi, Antonio Varone, Cedric Hubeau, Hyun-Hee Lee, Stephen E Alves, Michael Salmon, Thomas C Ferrante, James C Weaver, et al. Small airway-on-a-chip enables analysis of human lung inflammation and drug responses in vitro. Nature methods, 13(2):151–157, 2016.

[87] Trieu Nguyen, Dang Duong Bang, and Anders Wolff. 2019 novel coronavirus disease (covid-19): paving the road for rapid detection and point-of-care diagnostics. Micromachines, 11(3):306, 2020.

[88] Juan Eduardo Sosa-Hernández, Angel M Villalba-Rodríguez, Kenya D. Romero-Castillo, Mauricio A Aguilar-Aguila-Isaías, Isaac E García-Reyes, Arturo Hernández-Antonio, Ishtiaq Ahmed, Ashutosh Sharma, Roberto Parra-Saldívar, and Hafiz M.N. Iqbal. Organs-on-a-chip module: A review from the development and applications perspective. Micromachines, 9, 2018.

[89] Neda Azizipour, Rahi Avazpour, Derek H. Rosenzweig, Mohamad Sawan, and Abdellah Ajji. Evolution of biochip technology: A review from lab-on-a-chip to organ-on-a-chip. Micromachines, 11, 2020.

[90] Kyung-Jin Jang and Kahp-Yang Suh. A multi-layer microfluidic device for efficient culture and analysis of renal tubular cells. Lab on a Chip, 10(1):36–42, 2010.

[91] Kyung-Jin Jang, Ali Poyan Mehr, Geraldine A Hamilton, Lori A McPartlin, Seyoon Chung, Kahp-Yang Suh, and Donald E Ingber. Human kidney proximal tubule-on-a-chip for drug transport and nephrotoxicity assessment. Integrative Biology, 5(9):1119–1129, 2013.

[92] Samira Musah, Nikolaos Dimitrakakis, Diogo M Camacho, George M Church, and Donald E Ingber. Directed differentiation of human induced pluripotent stem cells into mature kidney podocytes and establishment of a glomerulus chip. Nature protocols, 13(7):1662–1685, 2018.

[93] Martijn J Wilmer, Chee Ping Ng, Henriëtte L Lanz, Paul Vulto, Laura Suter-Dick, and Rosalinde Masereeuw. Kidney-on-a-chip technology for drug-induced nephrotoxicity screening. Trends in biotechnology, 34(2):156–170, 2016.

[94] Mengying Zhou, Xulang Zhang, Xinyu Wen, Taihua Wu, Weidong Wang, Mingzhou Yang, Jing Wang, Ming Fang, Bingcheng Lin, and Hongli Lin. Development of a functional glomerulus at the organ level on a chip to mimic hypertensive nephropathy. Scientific reports, 6(1):31771, 2016.

[95] Samira Musah, Akiko Mammoto, Thomas C Ferrante, Sauveur SF Jeanty, Mariko Hirano-Kobayashi, Tadanori Mammoto, Kristen Roberts, Seyoon Chung, Richard Novak, Miles Ingram, et al. Mature induced-pluripotent-stem-cell-derived human podocytes reconstitute kidney glomerular-capillary-wall function on a chip. Nature biomedical engineering, 1(5):0069, 2017.

[96] Tom TG Nieskens and Anna-Karin Sjögren. Emerging in vitro systems to screen and predict drug-induced kidney toxicity. In Seminars in nephrology, volume 39, pages 215–226. Elsevier, 2019.

[97] Ji Wang, Cheng Wang, Na Xu, Zheng-Fei Liu, Dai-Wen Pang, and Zhi-Ling Zhang. A virus-induced kidney disease model based on organ-on-a-chip: Pathogenesis exploration of virus-related renal dysfunctions. Biomaterials, 219:119367, 2019.

[98] Roberta Visone, Mara Gilardi, Anna Marsano, Marco Rasponi, Simone Bersini, and Matteo Moretti. Cardiac meets skeletal: what's new in microfluidic models for muscle tissue engineering. Molecules, 21(9):1128, 2016.

[99] Anna Grosberg, Alexander P Nesmith, Josue A Goss, Mark D Brigham, Megan L McCain, and Kevin Kit Parker. Muscle on a chip: in vitro contractility assays for smooth and striated muscle. Journal of pharmacological and toxicological methods, 65(3):126–135, 2012.

[100] Donghui Zhang, Ilya Y Shadrin, Jason Lam, Hai-Qian Xian, H Ralph Snodgrass, and Nenad Bursac. Tissue-engineered cardiac patch for advanced functional maturation of human esc-derived cardiomyocytes. Biomaterials, 34(23):5813–5820, 2013.

[101] Yu Shrike Zhang, Andrea Arneri, Simone Bersini, Su-Ryon Shin, Kai Zhu, Zahra Goli-Malekabadi, Julio Aleman, Cristina Colosi, Fabio Busignani, Valeria Dell'Erba, et al. Bioprinting 3d microfibrous scaffolds for engineering endothelialized myocardium and heart-on-a-chip. Biomaterials, 110:45–59, 2016.

[102] Xi Zhang, Tianxing Wang, Ping Wang, and Ning Hu. High-throughput assessment of drug cardiac safety using a high-speed impedance detection technology-based heart-on-a-chip. Micromachines, 7(7):122, 2016.

[103] Anna Marsano, Chiara Conficconi, Marta Lemme, Paola Occhetta, Emanuele Gaudiello, Emiliano Votta, Giulia Cerino, Alberto Redaelli, and Marco Rasponi. Beating heart on a chip: a novel microfluidic platform to generate functional 3d cardiac microtissues. Lab on a Chip, 16(3):599–610, 2016.

[104] Oliver Schneider, Lisa Zeifang, Stefanie Fuchs, Carla Sailer, and Peter Loskill. User-friendly and parallelized generation of human induced pluripotent stem cell-derived microtissues in a centrifugal heart-on-a-chip. Tissue Engineering Part A, 25(9-10):786–798, 2019.

[105] Evangeline Tzatzalos, Oscar J Abilez, Praveen Shukla, and Joseph C Wu. Engineered heart tissues and induced pluripotent stem cells: macro-and microstructures for disease modeling, drug screening, and translational studies. Advanced drug delivery reviews, 96:234–244, 2016.

[106] Seungkuk Ahn, Herdeline Ann M Ardoña, Johan U Lind, Feyisayo Eweje, Sean L Kim, Grant M Gonzalez, Qihan Liu, John F Zimmerman, Georgios Pyrgiotakis, Zhenyuan Zhang, et al. Mussel-inspired 3d fiber scaffolds for heart-on-a-chip toxicity studies of engineered nanomaterials. Analytical and bioanalytical chemistry, 410:6141–6154, 2018.

[107] Ken-ichiro Kamei, Yoshiki Kato, Yoshikazu Hirai, Shinji Ito, Junko Satoh, Atsuko Oka, Toshiyuki Tsuchiya, Yong Chen, and Osamu Tabata. Integrated heart/cancer on a chip to reproduce the side effects of anti-cancer drugs in vitro. RSC advances, 7(58):36777–36786, 2017.

[108] Anne M Taylor, Mathew Blurton-Jones, Seog Woo Rhee, David H Cribbs, Carl W Cotman, and Noo Li Jeon. A microfluidic culture platform for cns axonal injury, regeneration and transport. Nature methods, 2(8):599–605, 2005.

[109] Anja Kunze, Michele Giugliano, Ana Valero, and Philippe Renaud. Micropatterning neural cell cultures in 3d with a multi-layered scaffold. Biomaterials, 32(8):2088–2098, 2011.

[110] Jaewon Park, Sunja Kim, Su Inn Park, Yoonsuck Choe, Jianrong Li, and Arum Han. A microchip for quantitative analysis of cns axon growth under localized biomolecular treatments. Journal of neuroscience methods, 221:166–174, 2014.

[111] Onur Kilic, David Pamies, Emily Lavell, Paula Schiapparelli, Yun Feng, Thomas Hartung, Anna Bal-Price, Helena T Hogberg, Alfredo Quinones-Hinojosa, Hugo Guerrero-Cazares, et al. Brain-on-a-chip model enables analysis of human neuronal differentiation and chemotaxis. Lab on a Chip, 16(21):4152–4162, 2016.

[112] Stephanie Dauth, Ben M Maoz, Sean P Sheehy, Matthew A Hemphill, Tara Murty, Mary Kate Macedonia, Angie M Greer, Bogdan Budnik, and Kevin Kit Parker. Neurons derived from different brain regions are inherently different in vitro: a novel multiregional brain-on-a-chip. Journal of neurophysiology, 117(3):1320–1341, 2017.

[113] Javier Bustamante Mamani, Bruna Souto Marinho, Gabriel Nery de Albuquerque Rego, Mariana Penteado Nucci, Fernando Alvieri, Ricardo Silva dos Santos, João Victor Matias Ferreira, Fernando Anselmo de Oliveira, and Lionel Fernel Gamarra. Magnetic hyperthermia therapy in glioblastoma tumor on-a-chip model. Einstein (São Paulo), 18:eAO4954, 2020.

[114] Uwe Marx, Heike Walles, Silke Hoffmann, Gerd Lindner, Reyk Horland, Frank Sonntag, Udo Klotzbach, Dmitry Sakharov, Alexander Tonevitsky, and Roland

Lauster. 'human-on-a-chip'developments: a translational cutting-edge alternative to systemic safety assessment and efficiency evaluation of substances in laboratory animals and man? Alternatives to laboratory animals, 40(5):235–257, 2012.

[115] Ahmad Rezaei Kolahchi, Nima Khadem Mohtaram, Hassan Pezeshgi Modarres, Mohammad Hossein Mohammadi, Armin Geraili, Parya Jafari, Mohsen Akbari, and Amir Sanati-Nezhad. Microfluidic-based multi-organ platforms for drug discovery. Micromachines, 7(9):162, 2016.

[116] Hasan Erbil Abaci and Michael L Shuler. Human-on-a-chip design strategies and principles for physiologically based pharmacokinetics/pharmacodynamics modeling. Integrative Biology, 7(4):383–391, 2015.

[117] Boyang Zhang, Miles Montgomery, M Dean Chamberlain, Shinichiro Ogawa, Anastasia Korolj, Aric Pahnke, Laura A Wells, Stéphane Massé, Jihye Kim, Lewis Reis, et al. Biodegradable scaffold with built-in vasculature for organ-on-a-chip engineering and direct surgical anastomosis. Nature materials, 15(6):669–678, 2016.

[118] Kacey Ronaldson-Bouchard and Gordana Vunjak-Novakovic. Organs-on-a-chip: a fast track for engineered human tissues in drug development. Cell stem cell, 22(3):310–324, 2018.

[119] Laetitia Shintu, Régis Baudoin, Vincent Navratil, Jean-Matthieu Prot, Clément Pontoizeau, Marianne Defernez, Benjamin J Blaise, Céline Domange, Alexandre R Péry, Pierre Toulhoat, et al. Metabolomics-on-a-chip and predictive systems toxicology in microfluidic bioartificial organs. Analytical chemistry, 84(4):1840–1848, 2012.

[120] Leila Choucha-Snouber, Caroline Aninat, Laurent Grsicom, Geoffrey Madalinski, Céline Brochot, Paul Emile Poleni, Florence Razan, Christiane Guguen Guillouzo, Cécile Legallais, Anne Corlu, et al. Investigation of ifosfamide nephrotoxicity induced in a liver–kidney co-culture biochip. Biotechnology and bioengineering, 110(2):597–608, 2013.

[121] Paul M van Midwoud, Marjolijn T Merema, Elisabeth Verpoorte, and Geny MM Groothuis. A microfluidic approach for in vitro assessment of interorgan interactions in drug metabolism using intestinal and liver slices. Lab on a Chip, 10(20):2778–2786, 2010.

[122] Thibault Bricks, Patrick Paullier, Audrey Legendre, Marie-José Fleury, Perrine Zeller, Franck Merlier, Pauline M Anton, and Eric Leclerc. Development of a new microfluidic platform integrating co-cultures of intestinal and liver cell lines. Toxicology in Vitro, 28(5):885–895, 2014.

[123] Ilka Maschmeyer, Tobias Hasenberg, Annika Jaenicke, Marcus Lindner, Alexandra Katharina Lorenz, Julie Zech, Leif-Alexander Garbe, Frank Sonntag, Patrick Hayden, Seyoum Ayehunie, et al. Chip-based human liver–intestine and liver–skin co-cultures–a first step toward systemic repeated dose substance testing in vitro. European journal of pharmaceutics and biopharmaceutics, 95:77–87, 2015.

[124] Gordana Vunjak-Novakovic, Sangeeta Bhatia, Christopher Chen, and Karen Hirschi. Heliva platform: integrated heart-liver-vascular systems for drug testing in human health and disease. Stem cell research & therapy, 4(1):1–6, 2013.

[125] Ilka Maschmeyer, Alexandra K Lorenz, Katharina Schimek, Tobias Hasenberg, Anja P Ramme, Juliane Hübner, Marcus Lindner, Christopher Drewell, Sophie Bauer, Alexander Thomas, et al. A four-organ-chip for interconnected long-term co-culture of human intestine, liver, skin and kidney equivalents. Lab on a Chip, 15(12):2688–2699, 2015.

[126] T Satoh, S Sugiura, K Shin, R Onuki-Nagasaki, S Ishida, K Kikuchi, M Kakiki, and T Kanamori. A multi-throughput multi-organ-on-a-chip system on a plate formatted pneumatic pressure-driven medium circulation platform. Lab on a Chip, 18(1):115–125, 2018.

[127] Camilla Luni, Elena Serena, and Nicola Elvassore. Human-on-chip for therapy development and fundamental science. Current opinion in biotechnology, 25:45–50, 2014.

[128] Ulrich S Schwarz and Ilka B Bischofs. Physical determinants of cell organization in soft media. Medical engineering & physics, 27(9):763–772, 2005.

[129] Douglas B Weibel and George M Whitesides. Applications of microfluidics in chemical biology. Current opinion in chemical biology, 10(6):584–591, 2006.

[130] Camilla Luni, Hope C Feldman, Michela Pozzobon, Paolo De Coppi, Carl D Meinhart, and Nicola Elvassore. Microliter-bioreactor array with buoyancy-driven stirring for human hematopoietic stem cell culture. Biomicrofluidics, 4(3), 2010.

[131] Spatial Filters Gaussian Smoothing.

Appendix A

Soft Lithography

A.1 Method and Equipment

- Sylgard 184 Silicone Elastomer Kit PDMS (Contains the silicon elastomer base and the silicon elastomer curing agent)
- High Precision Balance
- Weighing Boat
- Pipette Tips
- Pipette
- Desiccator
- Vacuum Pump
- Mold
- Oven
- Tinfoil
- Resin
- Blade

A.2 Procedure

1. Place the weighing boat up to the high precision balance.
2. Use the pipette to transfer the Silicon elastomer base into the weighting boat.
3. Calculate 27ml of base.
4. Use the pipette to transfer 2.7ml of curing agent into the weighting boat.
5. Write down the total grams of the PDMS,
6. Use a pipette tip to mix well the base and the curing agent in a way that more bubbles will be created.

7. Place the weighting boat into the desiccator.
8. Place the tube connected with the vacuum pump on the desiccator's input.
9. Close the desiccator's valve.
10. Switch on the vacuum pump and open little by little the desiccator's valve till it is fully open.
11. Wait till the bubbles disappear from the PDMS.
12. While waiting for the PDMS in the desiccator, fold the tinfoil so it can support the mold with the PDMS.
13. When no bubbles are visible, close the valve of the desiccator.
14. Switch off the vacuum pump.
15. Open little by little the valve again so the atmospheric air can pass through.
16. Pour carefully the PDMS into the mold.
17. Remove any air bubbles with the pipette.
18. Place the mold with the PDMS in the oven and set the temperature to 50°C
19. Remove the PDMS from the oven after a day or more.
20. Use a blade to remove the PDMS from the mold.
21. Cut off each design.

Appendix B

Device Assembly

During the device assemble we put every part of the device together and made sure that everything was well attached. In order to have stronger bonding between the different parts we used the plasma surface treatment technique.

Plasma is considered the fourth state of the matter, and it is actually an ionized gas that consist from ions and electrons. During the plasma treatment the ionized gas modifies the properties of the material's surface. The plasma breaks the bonds in the material's surface making the attachment and bonding with other molecules easier. It is important to note that plasma is an efficient way to modify the properties of the surface without altering the materials characteristics in a larger scale.

B.1 Procedure

1. Create holes in the vacuum chamber in the bottom end of the "T" in both of the layer.
2. Create holes in both of the ends of the central channels in each layer
3. Place into the plasma surface treatment machine for 3 minute,the PDMS's bottom layer upside down (with the channels looking downwards) and the glass slide.
4. Then place into the glass slide the PDMS layer with the channel looking upwards.
5. Next, cut the porous membrane thin enough to cover the central channel into a rectangle shape.
6. Place the membrane and the PDMS-glass slide into plasma for another 3 minutes.
7. Then, place the treated side of the membrane on the central channel of the PDMS-glass slide.
8. Place into the plasma for 3 minutes the membrane-PDMS-glass slide and the PDMS top layer(with the channels looking upward).
9. Then, put the PDMS top layer on the top of the membrane-PDMS-glass slide and make sure the channels are aligned.
10. Lastly, place the device in the oven for a day, for everything to bond properly.

Appendix C

Arduino script

```
 /** This is the code for the Gut on a Chip project **/

void setup() {
  //runs once
  pinMode(4, OUTPUT);
  pinMode(LED_BUILTIN, OUTPUT);
  Serial.begin(9600);
}

void loop() {
  //runs repeatedly
  //sent a pulse to vacuum controler & switch on the led
  digitalWrite(4, HIGH);
  digitalWrite(LED_BUILTIN, HIGH);
  delay(6000);
  //zero signal, switch off the led
  digitalWrite(4, LOW);
  digitalWrite(LED_BUILTIN, LOW);
  delay(60000);
}
```

Appendix D

Image Analysis script

```
global imgsColumns imgsRows v sigma k;
global smallestdist largestdist  smallestframe largestframe folderNam

dispInfo();
[file,path]= uigetfile(".avi .mp4", "Select a video:");

if file==0
   disp("You must select a file to proceed. Run the program again!");
   return;
end

filename = fullfile(path, file);
%set sigma
  sigma=input("Give value for sigma:");
%load and read the video
video = VideoReader(filename);
numofframes= video.NumFrames;
framesDistance= zeros(2, numofframes);
firstframe=read(video, 1);
findDimensions(firstframe);

%create video with the edges
dateTime= datetime("now", 'Format','dd-MM-yyyy_HH:mm:ss');
dateTimestr= string(dateTime);
folderName= video.Name+"_results";
if ~exist(folderName, 'dir');
    mkdir(folderName);
end
filename= folderName+"/egdes_sigma="+sigma+"_"+ dateTimestr+".avi"
v = VideoWriter(filename);
open(v);

% find distances for each frame
smallestdist=10000000; % random number
largestdist=0;
smallestframe=0;
largestframe=0;
```

```
header=["frame" "1st wall col" "2nd wall col" "distance"];
writematrix( header, folderName+"walls_sigma="+sigma+".xlsx");
initialFrame = read(video, 1);
results=zeros(numofframes, 4);
for k = 1 : numofframes
    frame = read(video, k);
    dist=findDistance(frame);
end
modev= mode(results());
for r=1:numofframes
  modeDiff= (abs(results(r,2)-modev(2))*100)/modev(2);

  if(modeDiff>10)
    results(r,2)="x";
    results(r,3)="x";
    results(r,4)="x";
  else
      if(results(r,4)<smallestdist)
          smallestdist=results(r,4);
          smallestframe= r;
      end
      if results(r,4)>largestdist
         largestdist=results(r,4);
         largestframe= r;
     end

  end

end
disp("smallestframe "+smallestframe);
disp("largestframe" +largestframe);
smallestImageFrame= read(video, smallestframe);
imwrite(smallestImageFrame, "smallestFrame.png");
largestImageFrame= read(video, largestframe);
imwrite(largestImageFrame, "largestFrame.png");
close(v); % closing the video
calculatePercentage(video.Name);

function calculatePercentage(videoName)
    global sigma smallestdist largestdist  smallestframe largestframe
    excelName=videoName +"_results.xlsx";

    difference= largestdist- smallestdist;
    percentageChange= round(((difference*100)/smallestdist), 2);
    values= [sigma smallestdist  smallestframe largestdist largestfram

    if ~exist(excelName, 'file')
        header=["Sigma" "Smallest dist"  "Frame s/d"  "Largest dist"
        writematrix( header, excelName);
        writematrix( values, excelName', 'WriteMode','append');
```

```
    else
        T = readtable(excelName);
        [rows, columns]=size(T);
        latestrow=rows+2;
        range= "A"+latestrow+":F"+latestrow;
        writematrix( values, excelName, 'WriteMode','append');

    end
end

function findDimensions(img)
    global imgsColumns imgsRows;
    [rows, columns, depth]= size(img);
    imgsRows= rows;
    imgsColumns=columns;

end

function distance=findDistance(img)
    global imgsColumns imgsRows v sigma k folderName results temp;
    grayscale= im2gray(img);
    smoothImage = imgaussfilt(grayscale,sigma);
    bw= imbinarize(smoothImage);
    [BW1,threshOut,Gx,Gy] = edge(bw,'sobel');
    if(k==1)
        imwrite(BW1, "edges_SIGMA="+sigma+".png");
    end
    frame= im2double(BW1);
    writeVideo(v,frame);

    % will iterate the half image to find the first wall
    % the column that has the largest gradient is the one that contai
    % the wall
    selectedColumn=1;
    sumOfSelectedCol=0;
    temp = [imgsColumns/2];
    for c=1: (imgsColumns/2)-1
        columnSum=0;
        for r=1: imgsRows-1
            columnSum=columnSum+ abs(Gx(r,c));
        end
        temp(c)=columnSum;
    end
    max=0;
    maxPosition=0;
    newSelection=false;
    for s=1: length(temp)
        %check the value
        if(temp(s)>max)
```

```
            if(maxPosition~=0)
                if(s>1 && maxPosition<length(temp)&& maxPosition>1)
                    if( (temp(s)+temp(s-1)+temp(s+1)) > max+ temp(max
                        newSelection=true;
                    else
                        newSelection=false;
                    end
                elseif(s==1)
                    if(maxPosition<length(temp) && temp(s)+temp(s+1)>
                        newSelection=true;
                    elseif(temp(s)>max)
                        newSelection=true;
                    else
                        newSelection=false;
                    end
                end
            else
                newSelection=true;
            end
        end

        if(newSelection)
                max=temp(s);
                maxPosition=s;
        end
        newSelection=false;
    end
    sumOfSelectedCol= max;
    selectedColumn= maxPosition;

    % find the second wall in the second half of the image
    secondSelectedColumn=1;
    secondSumOfSelectedCol=0;
    for c=(imgsColumns/2): imgsColumns-1
        columnSum=0;
        for r=1: imgsRows-1
            columnSum=columnSum+ abs(Gx(r,c));
        end
        if columnSum>secondSumOfSelectedCol
            secondSumOfSelectedCol= columnSum;
            secondSelectedColumn= c;
        end
    end
    % selection of the vertical half of the image, into the two colum
    % in order for the points to be paraller to find them distance

    distance =secondSelectedColumn-selectedColumn;

    temp=[k selectedColumn  secondSelectedColumn distance];
    writematrix( temp, folderName+"walls_sigma="+sigma+".xlsx", 'Write
```

```
    results(k,1)=k;
    results(k,2)=selectedColumn;
    results(k,3)= secondSelectedColumn;
    results(k,4)= distance;
end

function dispInfo()
    disp("Program requirements:");
    disp("The selected video should show the channel in vertical arran

end
```